1973

GRAIN BOUNDARY MOBILITY IN ANION DOPED MgO

DRA

By

Cawas M. Kapadia and Martin H. Leipold
Department of Metallurgical Engineering
and Materials Science
University of Kentucky
Lexington, Kentucky 40506

NGL-18-001-042

Abstract

Certain anions (OH^-, F^- and Cl^-) are shown to enhance grain growth in MgO. The magnitude of their effect decreases in the order in which the anions are listed and depends on their location (solid-solution, second phase) in the MgO lattice. As most anions exhibit relatively high vapor pressures at sintering temperatures, they retard densification and invariably promote residual porosity. The role of anions on grain growth rates has been studied in relation to their effect on pore mobility and pore removal; the atomic process controlling the actual rates has been determined from observed kinetics in conjunction with the microstructural features.

With respect to controlling mechanisms, the effects of all anions are not the same. OH^- and F^- control behavior through creation of a defect structure and a grain boundary liquid phase while Cl^- promotes matter transport within pores by evaporation-condensation. Studies on an additional anion, S^{2-} gave results which were no different from undoped MgO, possibly because of evaporative losses during hot pressing. Hence, the effect of sulphur is negligible or undetermined.

OUTLINE OF PAPER

I Introduction

II Theory

III Experimental Procedure

IV Results and Discussions

A - Undoped MgO

a) Grain growth in dense (≥99.4%) MgO of different porosities
b) Grain growth in Fisher (low purity)MgO with different densities.
   (i) More dense Fisher MgO (UK 132, 0.4% porosity)
   (ii) Less dense Fisher MgO (UK 130, 2% porosity)

B - Anion doped Fisher MgO

1) Fluorine (F) Doped Fisher MgO
2) Chlorine (Cl) Doped MgO
3) Sulphur (S) Doped MgO
4) Hydroxyl (OH) Doped MgO
   (i) $t^{\frac{1}{2}}$ dependence ($t < 1000$ mins.)
   (ii) $t^{\frac{1}{3}}$ dependence ($t > 2000$ mins.)

C - Comparison between Anions

V Summary and Conclusions

Introduction

Impurities are known to control the microstructure (grain size and related properties) of ceramic materials. It is clear that impurities tend to reside at grain boundaries in ceramics even in relatively high purity materials.[1, 2] Extensive work on role of impurities on grain growth kinetics has been reported,[3] but unfortunately all emphasis has been on cation additives. Anions in general have received little attention as specific impurities. This is in spite of the fact that there are numerous suggestions as to the phenomenological importance of anions in the literature. For example, flouride additions significantly enhance the fabricability of MgO by hot pressing.[4] Ceramic surfaces, qualitatively similar to grain boundaries show a strong affinity for gases (Cl_2, F_2, H_2O).[5, 6] One reason for lack of attention to anion impurities in ceramics is the analytical problems involved in their detection; routine survey analyses being insensitive to their presence. However, studies have clearly shown that they are present and do often exist as a major impurity when cation impurities are reduced to 0.01% or less.[7]

With the exception of water vapor,[8] few data are available concerning the influence of anions on grain growth in MgO. The purpose of the present work is to define the effect of anions on grain boundary migration in a typical ceramic oxide, MgO; the results here are expected to be applicable to all types of conventional ceramics. The choice of material (MgO) is based on a number of factors. Anions are known to have some effect on the fabricability of MgO and thus their presence in the material is to be expected. Also, the substantially ionic nature of MgO makes substitution of additives in the lattice or at grain boundaries more likely, as well as, providing a somewhat easier theoretical consideration of atomic substitution. Again, a great deal is known concerning grain boundary phenomena in other rock salt type materials, especially alkali halides and the results obtained here could be interpreted and compared with those of other workers.

The effect of anions on grain growth kinetics in MgO must be considered in light of their physical characteristics (e. g. solubility in the matrix, vapor pressure) which will determine the nature (form) in which they exist in the oxide (gaseous specie, precipitates or grain boundary liquid phase). Since most anions (as elements or as magnesium compounds) exhibit relatively high vapor pressures at temperatures of interest, an entrapped gas phase exists within the microstructure which retards densification giving invariably some residual porosity.[9] As pores are also known to control grain boundary migration rates, the role of anions themselves on grain growth must be studied in junction with their effect on intrinsic pore mobility and subsequent pore removal. This effect can be clearly defined if such pore controlled grain growth in undoped MgO is compared with that in anion doped material and toward that end, such investigations are included here.

II. Theory

A brief review of grain growth theory relating rate controlling mechanisms to relevant microstructural features is essential and is discussed here. The theory of grain boundary migration in real ceramics must take into account various modifications due to material factors such as porosity and second phase particles. According to basic theory of grain growth in polycrystals,[10] the growth rate depends strictly on boundary curvature and is given by

$$\frac{dD}{dt} = \frac{K}{D} \tag{1}$$

where K is the temperature dependent rate constant and D is average grain size at anneal time t. On integration equation (1) becomes

$$D^2 - D_o^2 = Kt \tag{2}$$

where D_o is grain size at $t = 0$. When grain growth inhibiting effects are present, the growth law is empirically represented by

$$D^n - D_o^n = Kt \tag{3}$$

or if $D >> D_o$,

$$D^n = Kt \tag{4}$$

where the grain growth exponent (n) more commonly observed is greater than the theoretically predicted value of 2. Since equation (4) can be written as $D = Kt^{1/n}$, growth exponent (n) corresponds to $t^{1/n}$ time dependence of grain growth.

The square growth law (n = 2) in equation (2) has been observed for zone-refined metals[11] and fully dense MgO.[12] On the other hand, for porous MgO, grain boundary velocity is controlled by

(i) pore removal (simultaneous densification) for interconnected porosity ($\gtrsim 5\%$) with n = 2, and

(ii) pore mobility for isolated pores lying along the grain boundaries (porosity $\lesssim 5\%$) where $n \geq 2$.

Thus, in the presence of porosity, n may or may not equal 2, and when n = 2, the controlling mechanism could differ. Since most compacts in

this study were hot pressed well into the final stage of densification, the latter case is of primary significance here.

For such latter stages, isolated pores at grain boundaries are expected to be the controlling type, and the pores migrate with the boundary with velocity (V) given by [13]

$$V = \frac{M_b F_b}{1 + NM_b/M_p} \tag{5}$$

where M_b is intrinsic grain boundary mobility, M_p the average pore mobility, F_b the total force driving the motion of the average grain boundary and N the average number of pores per boundary. As a first approximation, it is assumed that $V \propto dD/dt$, $M_b \propto \exp\left(\frac{-Q_G}{RT}\right)$, $F_b \propto (4\gamma_{GB}/D)S$, $M_p \propto \frac{1}{r^m}$, $r \propto D$ and $S \propto D^2$, where dD/dt is the average grain growth rate, Q_G is activation energy of boundary migration, γ_{GB} is the specific grain boundary energy, S is the area of the average grain boundry, r is the average pore radius and m is integer depending on mechanism of material transport responsible for pore migration[14]. Equation (5) reduces to two important forms depending on relative magnitudes of M_b and M_p.[13] These are

(i) $V = M_b F_b$ when $M_p >> NM_b$ and corresponds to grain growth controlled by boundary mobility alone,

(ii) $V = M_p F_b/N$ when $M_p << NM_b$ for pore controlled growth.

Table I summarizes these two cases together with the physical conditions when each is expected to be applicable.

For Case (i), where boundary mobility is rate-controlling, the impurities in the material influence grain boundary velocity by controlling both M_b and F_b depending on their location (grain boundary vs grain interior) and their form in the matrix namely: solid solution, discontinuous second phase (precipitate) and continuous boundary phase (which could be a liquid at annealing temperature). The mechanism that controls grain growth in each case is different but in general gives cubic kinetics (n = 3).[15, 16] These rate controlling processes are:

a) Extrinsic grain boundary mobility (solute dragging). No single law is obeyed though n = 3 is most often suggested.

b) Viscous drag of discontinuous second-phase inclusion. Inclusion coalescence is rate controlling and a $t^{\frac{1}{3}}$ grain growth law is obeyed if material is transferred from one inclusion to another via volume diffusion while a $t^{\frac{1}{4}}$ law for material transfer by grain boundary diffusion.[17]

c) Material transfer across a continuous boundary liquid phase. ($\gamma_{GB} > 2\gamma_{LS}$). If diffusion through the boundary phase is rate controlling (driving force being concentration gradient of diffusing specie) the growth law is $t^{\frac{1}{3}}$ whilst, if surface reaction at the liquid-solid interface is controlling, $t^{\frac{1}{2}}$ dependence is observed.[18] Also, the growth rate is usually found to depend on the amount of liquid phase.

For case (ii) corresponding to pore mobility control, the boundary velocity can be expressed in terms of N and D as

$$\frac{dD}{dt} = \frac{M_p F_b}{N} \propto \frac{1}{D^m} \frac{D}{N} \approx \frac{1}{ND^{m-1}} \qquad (6)$$

If $N \propto f(\frac{D}{r})^3$ where f = volume fraction of randomly dispersed intergranular pores, then assuming f = constant and $r \propto D$,[19] we have N = constant which will be true if pores existed only at boundary intersections (grain corners).[13,16] In such a situation, integration of equation (6) gives

$$D^m - D_o^m = Kt$$

However, one expects some densification during grain growth (hence, f decreases) and since sweeping of pores along with grain boundaries require pore coalescence,[19] N should decrease with grain growth. Hence, a convenient assumption often made is $N \propto \frac{1}{D}$ which is appropriate for pores on individual grain boundaries.[13] Equation (6) then reduces to $dD/dt \approx 1/D^{m-2}$ which on integration gives

$$D^{m-1} - D_o^{m-1} = Kt \qquad (7)$$

Hence, depending on mode of material transport during pore migration (i.e. value of m) we get essentially two sets of grain growth exponents (n) namely, n = m for pores at boundary intersections and n = m-1 for pores on individual grain boundaries.[20] Since pores acutally lie both on grain boundaries and at triple points (boundary intersections), the above two cases of pore location by themselves may be somewhat idealized and one could actually observe an intermediate behavior. Table II gives values of n predicted for both cases of pore location, for each pore transport mechanism. Although one normally expects n > 2 for pore controlled grain growth, there are certain pore transport mechanisms wherein $n \leq 2$ is predicted. Further, since more than one transport mechanisms may be operating at the same time, experimental values of n may not always correspond to any single theoretical prediction. Also, very often a transient value of n = 3 (cubic growth kinetics) is reported in presence of porosity; this can be interpreted as n changing from a lower to a higher value (over a limited range of annealing time) behavior observed when pore migration probably occurs either by volume diffusion (across or around the pore) or by vapor transport with a constant pressure inside the pore.[20]

The above discussion was based on 1/D dependence of the driving force which is true when $D << r/f$. However, for large D, the driving force for grain growth is actually proportional to $(1/D - f/r)$.[21] As annealing progresses (D increases), inhibiting effect of pores become more pronounced till eventually grains cease to grow when

$$D \approx \frac{r}{f} \tag{8}$$

Limiting grain size $(GS)_L$ is said to have been reached and corresponds to value $n = \infty$. According to Haroun-Budworth,[22] for random dispersion of pores with inhibition by those at grain boundaries

$$(GS)_L \cong 0.15 \ \frac{r}{f} \tag{9}$$

The effectiveness of pore control on grain growth in MgO depends on annealing temperature; at high temperatures (~ 1500°C) pore inhibition is observed at very small annealing times. Limiting grain size may be reached after only a few hours since a rapid increase in D satisfies criterion(8) for limited growth. On the other hand, at lower temperatures (1300°C) where the grain growth rate is lower, pore control and growth limiting effects are important only at very large anneal times. (See Table I). In fact at such high anneal times, pore coalescence (increase in r) and simulataneous densification (reduction in f) may increase $(GS)_L$ to a value high enough that limiting grain size may not even be observed during normal sintering times. Also, at a given annealing temperature, changes in microstructure with time can give more than one kind of growth kinetics (different n values) over the whole annealing period. At a temperature like 1500°C when limiting grain size is observed, one expects to see further grain growth if annealing is continued. This is probably due to coalescence of intergranular pores and a decrease in volume fraction porosity, both of which give a higher value of $(GS)_L$. On the other hand, it is possible that given sufficient time, thermal fluctuations may provide grain boundaries "anchored" by the less mobile pores sufficient energy to overcome restraining effect of pores and break free thus, including them within the grain. This will lead to further grain growth unaffected by pores, with a microstructure consisting of very large isolated crystals in a matrix of fine uniformly sized grains. This situation is commonly referred to as secondary or exaggerated grain growth and probably arises from inhomogeneous pore distribution.

In conclusion, grain growth kinetics is influenced by the presence of porosity and impurities. A combination of mechanisms of comparable importance involving pore-grain boundary interactions may operate simultaneously in which case time-dependence of grain growth is insufficient to determine the atomic processes which control rate of grain growth and change in pore size. Only by observations of microstructure

and its change with time, can one eliminate alternate hypotheses and determine the rate controlling process or processes under particular conditions. In the present study, microstructural features of both pure and anion doped MgO are investigated and used as a basis for interpreting the grain growth behavior.

III. Experimental Procedure

Grain growth anneals were done for two types of hot pressed MgO compacts.

1) Undoped wherein two grades of initial magnesia powder were used: High Purity JPL MgO and Fisher M-300 electronic grade. The preparation of JPL MgO, chemical analysis of both grades and hot pressing conditions are given in an earlier paper.[23] The Fisher was used because of its ready availability and impurity levels which are typical of commercial magnesia.

2) Doped wherein known amounts of S^{-2}, Cl^-, OH^-, OD^-, F^- are added to Fisher M-300 electronic grade MgO. Sources of these anions, equipment, hot-pressing techniques and chemical analysis of as pressed specimens are given in Reference (9). The OD^- was chosen as an anion impurity not because it was expected to differ in behavior from OH^- but because its use would clearly differentiate between the additive and contamination from the laboratory atmosphere. However, efforts to quantitate OD^- gave negative results (apparently exchange with an unknown source occurred) and no grain growth results on OD^- doped MgO can be reported.

Grain growth anneals were done at 1300°C and 1500°C (temperature selection was based on convenience) under air atmosphere in conventional Al_2O_3 muffle tube furnace with SiC heating elements. The furnace temperature was measured by a Pt/Pt-10% Rh thermocouple within $\pm$ 10%. Annealing times ranged from 10 minutes to a week. After each time interval the specimens were removed from the furnace, examined microscopically, photographed and returned to the furnace for continued annealing. To get an average behavior, different polished sections were examined after each anneal. New surfaces were sectioned, polished conventionally[24] and etched and average grain size was determined within $\pm$ 10% by lineal analysis, as described by Hilliard.[25] Table III gives characteristics of hot-pressed specimens used in these studies; reported bulk densities taken by kerosene displacement do not consider any variation within a specimen.

IV. Results and Discussions

This part is divided into 3 sections: (A) Preliminary grain growth study on undoped Fisher MgO of varying porosity to determine relative importance of pores and impurity; (B) a discussion on anion doped Fisher MgO and finally (C) a comparison between these studies to reveal any effect, if at all, of the anions on boundary migration.

A - Undoped MgO

To clearly bring out the influence of anions alone on pore and grain boundary mobility, it was necessary to separate their effect from that of inherent cation impurities (Ca^{2+}, Si^{4+}, Al^{3+}, Fe^{2+}) in Fisher MgO. Hence, to study influence of these cations (~1000 ppm), grain growth in Fisher MgO is first compared with that in JPL MgO which has a much lower cation impurity content (< 200 ppm). Further, to determine whether grain growth kinetics is sensitive to different levels of porosity, studies were also conducted on undoped Fisher MgO (less pure) with two different porosities.

(a) Grain growth in dense (≥ 99.4%) MgO of different purities

Data at 1300°C and 1500°C for dense MgO specimens of both purities is given in Figure 1.

1300°C.

High purity JPL MgO (OP373 and OP356) gave n = 2 which corresponds to normal uninhibited growth. Only OP373 (slightly less dense than OP356) showed small pores in the microstructure and these were mobile enough so as not to give appreciable drag on moving grain boundaries ($M_p > M_b$). On the other hand microstructure of less pure Fisher MgO (HP332) showed considerable liquid phase (probably Ca-Si rich phase and Al-rich phase) at triple points and grain boundaries due to cation segretation[1]; a value of n = 3, corresponding to grain growth in presence of liquid phase was accordingly observed. We can conclude that at 1300°C, in spite of slightly different densities, both high purity specimens gave n = 2; the less pure Fisher gave n = 3. Hence, difference

in behavior is based on impurity levels and not densities.

1500°C

Behavior between fully dense, pure MgO (OP356) and 99.6% dense, less pure MgO (HP332) is compared. There are three regions, each of which have different microstructural features that determine grain growth kinetics.

(1) $t < 200$ mins.

Results directly compare to the lower temperature behavior for the pure OP356, $n = 2$ corresponding to normal uninhibited grain growth while for HP332, presence of impurities mostly as grain boundary liquid phase gave $n = 3$.

(2) 200 mins. $< t <$ 1500 mins.

Both specimens exhibit limiting grain growth behavior with $(GS)_L \cong 70 \mu m$. This is due to presence of growth limiting inclusions like porosity and second phase observed in their microstructures. Such grain growth inhibition even for OP356 (theoretically dense, ultra pure MgO) suggests that even very slight amounts of porosity and second phase are capable of limiting grain boundary velocity. However, such limited growth in OP356 was observed for relatively shorter period than in less dense HP332.

(3) $t >$ 1500 mins.

Limiting grain growth over an order of magnitude in annealing time is followed by further uninhibited growth; this could be due to coalescence of intergranular inclusions (brought about by grain boundary dragging) together with a decrease in volume fraction porosity brought about by densification without appreciable grain growth.

As most porosity for less pure HP332 (Fisher material) was observed to be within individual grain (rather that on grain boundaries), grain boundaries initially anchored by the pores might be gradually separating themselves from their pinning inclusions during the constant grain size region giving rise to normal growth at large annealing times.

Again for t > 1500 mins., microstructure for very pure, dense MgO (OP356) showed no inclusions and n = 2 corresponding to intrinsic boundary controlled grain growth. On the other hand, n = 3 for less pure HP332 corresponding to material transfer across the grain boundary liquid phase. Briefly, in very dense and pure MgO, intrinsic boundary mobility controlled grain growth whilst for less pure material growth was impurity controlled. There was no evidence of secondary grain growth in both materials.

Comparing next, OP373 (high purity, 99.4% dense), with OP356 (high purity, fully dense) and HP332 (less pure, 99.6% dense), we see somewhat different behavior. No grain growth was observed for OP373 (secondary growth prevent valid data for the longest anneals); even after long anneals / limiting grain size $(GS)_L$ was reached only after an anneal of 1 hour. This is in contrast to grain growth and a larger $(GS)_L$ observed for OP356 (equivalent purity but zero porosity) and less pure HP332 of comparable porosity. It appears that in the less pure HP332, the cation impurities might have influenced pore mobility and also enhanced their removal by formation of eutectic (low melting) phase at grain boundary[1]. The limiting grain size $(GS)_L$ for OP373 at 1500°C is 55μ and is less than that for OP356 and HP332. Quantitative studies of optical micrographs gave average pore radius (r) between 2 and 2.5μm. As volume fraction porosity (f) is 0.006, $(GS)_L$ by equation (9) lies between 50 and 60μm. The agreement may be fortuitous and traces of second phase could still contribute slightly to limiting grain growth effects. As levels of porosity in OP356 (fully dense, very pure MgO) are extremely small compared to OP373 a higher value of $(GS)_L = 70\mu m$ is observed. Also, impurities in less pure Fisher MgO (HP332) gave boundary liquid phase which enhanced densification giving a higher $(GS)_L = 70\mu m$.

Briefly reviewing the relative influence of porosity and impurities, one concludes that (i) small amounts of porosity (<1/2%) are more detrimental to grain growth than small impurity levels in the material, in fact, presence of some impurities may even help reduce the hindering

effect of pores by modification of the pore phase in the microstructure.
(ii) Theoretically predicted square kinetics (n = 2) is indeed observed for fully dense, high purity MgO; however, for a short period at 1500°C limited (zero) growth was observed even in presence of negligible porosity and second phase.

(b) Grain growth in Fisher MgO (low purity) with different densities

To determine whether grain growth kinetics is sensitive to different levels of porosity, studies were conducted on undoped MgO with two different porosities. As anion doped MgO specimens also had two porosity levels namely (a) < 1/2% and (b) 1 - 4% porosity, any difference in behavior after anion addition with respect to the two porosity levels can be interpreted as a direct influence of the anions. In this section, undoped Fisher MgO with different porosities will be discussed.

Grain growth studies, (Figure 2) were done at 1300°C and 1500°C on two samples of Fisher MgO (UK132; 0.4% porosity) and (UK130; 2% porosity). These will be discussed separately.

(i) More dense Fisher MgO. (UK132; 0.4% porosity)
1300°C.

Typical microstructures showed few very fine pores along grain boundaries at small anneal times (< 600 mins.) whilst at larger heat treatments (1000-3000 mins.) large and hence, less mobile pores at grain boundaries, especially near triple points. Accordingly, observed kinetics was n = 2 (eqn. 3) up to 600 mins. (no pore influence) whilst as pore control became important, a cubic, n = 3 law up to 4000 mins. Microstructure showed no evidence of any boundary liquid phase, hence, pore removal was not very rapid and a limiting grain size is obtained at very long heat treatments. Considerable intragranular porosity observed in one week anneal specimens indicate that grain boundaries were beginning to free themselves from large, less mobile pores and trapping them inside the grains.

1500°C

Comparison of time dependence shows that limiting grain size at 1500°C is reached more rapidly and at a smaller grain size than at 1300°C for reasons discussed earlier in Part II. At 1500°C, an initial n = 2 behavior up to 150 mins. is followed by a constant grain size (70μ) up to 1000 mins. Photomicrographs only showed some intergranular pores at 600 mins. but they were accompanied by considerable liquid phase wetting at grain boundaries and triple points at 2000 mins. It is probable that liquid phase enhanced pore removal, thus reducing porosity to a very low level which resulted in uninhibited growth (n=2) after 1000 mins. It is not clear, however, whether intrinsic boundary mobility or surface reaction at solid-liquid interface was rate controlling at these long times. A simple calculation shows that considerable densification has indeed occurred. If in equation (9) $(GS)_L$ = 70μm and r_{max}(at 2000 mins.) = 1μm; the volume fraction (f) of porosity comes out to be 0.002 which means that at 2000 mins. porosity has been reduced by one-half (initial porosity was 0.4%). If second phase inclusions in impure Fisher MgO were mainly responsible for the observed $(GS)_L$ at 75μ, then an increase in grain growth rate at longer anneal times cannot be explained since the quantity of second phase would not be expected to decrease with time.

(ii) Less dense Fisher MgO (UK 130; 2% porosity).

At 1300°C, the behavior is identical to denser UK132 up to 600 mins. For t > 600 mins. considerable scatter in the data makes it difficult to predict any definite kinetics although n = 3 seems to be the most likely kinetics. Data at 1500°C is not sufficient to draw any conclusion other than that grain sizes are comparable to that for dense Fisher material, UK 132 at 1500°C. Hence, Fisher MgO material with different porosity levels yield comparable grain sizes at both 1300°C and 1500°C.

From study of Fisher MgO, it is observed that two identical materials with equivalent porosity and impurity levels, UK132 (n = 2) and HP332 (n = 3), can give a very different grain growth behavior, Hence, it is concluded

that grain growth data depend critically on impurity concentration and distribution and hence caution must be exercised in interpreting it. As slight differences in amount of grain boundary liquid phase or porosity in the material drastically changes grain growth kinetics, any model calculations and time-temperature interpretations must depend on detailed description of the microstructure. Several grain growth anneals have to be studied before a truly representative behavior can be obtained. Role of impurities in hindering or aiding grain growth depend on whether they exist as second phase inclusions (hinderance) or liquid phase wetting the grain boundaries in which case they help grain growth

B - Anion Doped Fisher MgO

Interpretation of the experimental data for anion doped material must be done 1) in light of the known physical properties of the anions (Table IV), 2) with respect to the overall evolution of the microstructure, and 3) possible effects on diffusional characteristics of the material. Exact location of these volatile impurities in the MgO lattice would also aid in explaining their effect on pore and grain boundary mobility. Considerations of the additive anion size compared to that of oxygen in MgO (Table IV) suggests that F^- and OH^- would be reasonably soluble, whereas Cl^- and S^{2-} would not. F^- and OH^- in solution will give defect structure on Mg lattice, thus enhancing diffusion of rate controlling specie. The question as to whether they would segregate to the grain boundaries or remain uniformly distributed throughout the lattice is not resolved at this time.

Cl^- and S^{2-}, if not capable of solution, would normally be expected to exist as second-phase precipitates or more likely as entrapped gas[9] (due to their volatile nature), both of which retard the grain growth process. The low levels of these impurities retained after hot pressing (Table III) are generally consistent with the conclusion. Optical microscopy did not reveal any appreciable second phase particles, and the presence of porosity suggests a gas phase as a likely site for these anions, especially

for S, which can exist in a gas phase as SO_2 or SO_3. Further, cation impurities in Fisher MgO are known to form eutectic (low melting) phases at grain boundaries[1]; it is possible that some of the anions may control formation of a liquid phase.

Due to inhomogenities in distribution of porosity and impurities in the material, considerable scatter in some data is observed; also, because of the numerous possible mechanisms, it is not definitive physically to simply present observed values of grain growth exponents, n, or activation energy of rate controlling process. Rather a qualitative description of the limiting processes is attempted based on experimental data and microstructural observations.

(1) Fluorine (F) Doped Fisher MgO

For all anion studies, Fisher MgO was used. Data for each anion was obtained at two different densities. As two temperatures were studied (1300°C and 1500°C), discussion for both densities is given for each temperature separately. Figure 3 gives the grain growth data for F doped Fisher MgO.

1300°C

For F110 (less dense) pores were found at grain boundaries and triple points. Pore dragging controlled grain growth, giving n = 3 which indicates pore motion probably occurs by volume diffusion or vapor transport (See Part II). For F114 (more dense), n = 2 up to a grain size of 150μ. Microstructures, revealed absolutely no porosity or second phase, which suggests that intrinsic boundary mobility might be controlling. Fine pores (less than 1μm. size), if present, are sufficiently mobile so as not to give appreciable boundary drag. For grain sizes > 150μ, n increases to 3.

1500°C

Data scatter for F110 (less dense) for anneal time less than 200 mins. makes prediction of grain growth kinetics difficult although a value of n = 2 is most likely. Beyond this initial period, presence of intergranular porosity gives inhibited growth (large n) up to 4000 mins. After further heat treatment, microstructure reveals very little porosity residing mainly in grain interior with second phase (mostly liquid phase) at grain boundaries and triple points. A value of n = 2 is observed and could correspond to grain boundary mobility controlling or, more consistent with observed microstructure, diffusion across the liquid phase.

In contrast, microstructure revealed no porosity at all for more dense F114 (99.6% as pressed density) for all heat treatments; however, liquid phase was evident at grain boundaries especially near the triple points. Absence of any inclusions (pores or solid second phase) gave boundary controlled growth (n = 2) over the whole range of annealing time. From the experimental data at both temperatures, one concludes that for F, grain growth rates are sensitive to porosity differences of one per cent in contrast to undoped material where such sensitivity was not observed.

A striking observation at 1500°C for F114 is the extremely large grain sizes and absence of any constant grain size plateau observed for undoped Fisher MgO (UK132) of comparable as pressed density (99.6%). As observed by other workers such behavior could be due to fluorine additions enhancing densification (either by formation of a liquid phase[26] or defects due to solution of F^- in the O^{2-} lattice[27]). This is supported here by complete absence of porosity (potentially growth inhibiting) even after long heat treatments. Feasible reactions between MgF_2, residual carbonate and other cation impurities in Fisher MgO open up a range of possible low melting phases. Moreover, Ca as an inherent impurity cation is known to extend stability range of hydroxide - carbonate melts.[28] Also, since formation of liquid at grain boundary could only follow

segregation of cations (e.g. Ca^{2+}) at grain boundaries, F^- in solid solution could be indirectly aiding liquid formation by creating lattice defects, thus increasing diffusion rates of these cations. Other authors[29] have also observed substantial grain growth in presence of F and have attributed this to enhanced diffusion along and across a grain boundary layer of fluoride rich phase (either solid or liquid).

(2) Chlorine (Cl) Doped MgO

The effect of Cl on microstructure is different from that of F; F doped MgO showed liquid phase at triple points and in general, low levels of porosity which was removed during the anneals. No evidence of appreciable liquid phase was present for Cl specimens and the pore phase was present even after sufficiently long anneals. The difference in behavior could be related to the size of the Cl^- ion (relative to that of O^{2-}) which precludes its substitution for oxygen; in which case it exists as entrapped gas which retards densification. Also, the melting point of MgF_2 and $MgCl_2$ (source of these anions in MgO) are 1396°C and 712°C respectively, while vapor pressures (at an arbitrary temperature of 1000°C) are $< 10^{-6}$ atm and 0.03 atm respectively (Table IV). Hence, it is expected that unlike MgF_2, $MgCl_2$ or any other complex oxychloride will be unstable at the sintering temperature and will dissociate into vapor phase which will reside as gas bubbles in the microstructure. This is evident in fabrication studies[9] where a residual porosity was present in Cl specimens and back pressures in die cavity were calculated to be about ten times those for F. In addition it has been reported[30] that some fluorides can speed the release of physically and chemically adsorbed H_2O and CO_2 by progressive spreading over grains. Hence, a possible effect of F additions could be to remove adsorbed H_2O and CO_2 in the early hot-pressing stages so that as-pressed specimens contain less entrapped grain boundary porosity so detrimental to grain growth. In view of the presence of residual porosity, grain growth in Cl doped specimens will be largely pore controlled; any direct effect of Cl, if at all present, would be on the

mobility of these pores.

1300°C

For less dense, Cl doped MgO (C48) no appreciable grain growth was observed up to 1000 mins. (Fig. 4) due to presence of growth inhibiting interconnected porosity. Once the porosity was reduced to a level where pore phase was discontinuous (mostly as intergranular pores), grain growth controlled by pore mobility was observed with value of the grain growth exponent(n) between 1 and 2. An explanation for such behavior is proposed, based on a vapor transport mechanism involving evaporation-condensation. (Secondary grain growth in porous BeO has also been reported[31] to give n = 1, though no evidence for such behavior was present here). C115, a denser specimen (99.6% dense) also gave n = 1 at 1300°C up to 300 mins. followed by square kinetics (n = 2) observed up to a grain size of 200μ. Microstructure revealed some intergranular pores (~ 1μm) which makes boundary mobility controlled grain growth less likely. Square kinetics (n = 2), often observed for uninhibited growth, is observed here even in presence of pores. A possible explanation at these high temperatures and large pore sizes (~ 4μ for C48) is that pores move with the boundary by evaporation-condensation mechanism previously suggested for UO_2[32] and Al_2O_3.[32] It has been shown (Part II) that if vapor transport is indeed rate-controlling, then value of $n \leq 2$ is possible. The possibility of enhancement of vapor transport of MgO by a chlorination reaction brought about by chlorine acting as a carrier, either in elemental form or as magnesium compound is suggested. Such transport reactions play an important role in the formation of some minerals[33] and are consistent with a possible vapor transport mechanism here. At very large heat treatments(> 3000 mins.), the grain size for the denser material (C115) appears to stabilize at 200μ. It is not clear at this time whether such limiting growth is due to specimen size effect or change in pore behavior. Microstructure observations revealed a sudden increase in fine intergranular porosity in this period; a possible reason could be

decomposition of some internal phase (carbonates and hydroxides inherently present in Fisher MgO) resulting in gases which on diffusion along grain boundaries leave behind some porosity.

1500°C

Microstructures indicated pores (3μ size) at grain boundaries (especially near triple points) and grain interiors for porous C48 (95.6% dense) which restrict boundary mobility giving only a very light increase in grain size($n \rightarrow \infty$) over the whole anneal period. On the other hand, in less porous C115 (99.6% dense) there was appreciable grain growth with $t^{\frac{1}{2}}$ time dependence (Figure 4); however, the actual growth rates seem to depend on the individual specimen studied (data points in Figure 4 (b) which correspond to same specimen are identified with same numerical subscript). As different pore densities were observed in each of these specimens (inhomogeneous pore distribution in hot-pressed material), it appears that larger grain sizes correspond to a lower pore content.

In conclusion, for Cl doped MgO, presence of pore phase controls the overall evolution of the microstructure; grain growth rates are sensitive to pore content (as observed for F) and a proposed mechanism behind migration of intergranular pores is vapor transport.

(3) - Sulphur Doped MgO

Because of its large ionic radius, S^{2-} is not expected to go into solution in the O^{2-} lattice; further, it cannot form simple compounds with Mg (for example MgS) since these are not very stable at sintering temperatures. Hence, it is expected that sulphur exists either as sulphur vapor or as an oxide (SO_2, SO_3) residing with the pores.[9]

1300°C

S 96 (97.6% dense) gave n = 2.2; typical microstructure showed extremely fine pores both on grain boundaries and within individual grains. However, the mobility of these extremely fine pores was sufficiently large so as not to hinder boundary mobility. For S134, a denser S

doped material (99.3% dense), more data was obtained and it is possible to describe square kinetics in the beginning followed by n = 3 at times > 1000 mins. Data is given in Figure 5.

1500°C

Boundary mobility was rate controlling (n = 2) at short grain growth anneals (200 mins.) for both S96 and S134. However, at grain size around 65μ, inclusions (suspected to be pores) severely inhibited boundary mobility and a very limited growth (large n) was observed for a period of 40 hours. After further heat treatment, the porosity being reduced to a low level, grain growth is resumed with $t^{\frac{1}{2}}$ time dependence; typical micrographs showed pores mostly within grains with pore free regions around the grain boundaries.

There was no evidence of any appreciable liquid phase at grain boundaries (other than amount normally expected in undoped Fisher MgO) due to the presence of sulphur; hence, densification was not enhanced (as observed for fluorine) but was controlled by intrinsic pore mobility. However, scanning electron micrographs of large grain specimens (48 hrs. anneal at 1500°C) showed second phase which could be precipitates which gave large contact angles at grain boundaries and triple points (no wetting observed). (Figure 6). Hence, it is possible that boundary migration here is controlled by second phase precipitates together with intergranular pores. However, the $t^{\frac{1}{2}}$ growth dependence observed for less dense, S 96 precludes drag of these second phase inclusions to be rate-controlling. Even though specimens S96 and S 134 had different densities (3.48 g/cc and 3.55 g/cc respectively), the actual grain sizes and grain growth behavior for both specimens were similar at both 1300°C and 1500°C. However, if density is significantly low, as for S 33 (3.42 g/cc), the grain sizes at 1500°C are distinctly smaller and porosity level is sufficiently high to give pore controlled growth (n = 2.5). (Figure 5).

As no densification enhancement was evident in presence of sulphur, residual porosity existed in the material to give primarily pore controlled growth. Grain sizes were in general smaller than those in presence of

other anion specimens of comparable as pressed densities and corresponded more with undoped Fisher material. Further, grain growth rates for S were not nearly as sensitive to slight porosity differences in starting material as observed for other anions.

(4) OH^- Doped MgO

Earlier studies[8] indicate that both sintering and grain growth in magnesia are greatly enhanced by presence of OH^- ion; however, only the temperatures around 1000°C were studied. Here, grain growth in OH^- doped MgO at temperatures greater than 1300°C is investigated. It is suggested[34] that solution of the hydroxide in MgO gives Mg lattice defects which increase the rate of all diffusion processes. Also, OH^- can exist as a liquid phase probably as $Ca(OH)_2$ (from Ca in Fisher MgO) which is stable at the sintering temperatures at internal pore pressures of 1000 psi or less.[35] If on the other hand, if OH^- exists in form of H_2O vapor it can hinder densification giving limiting porosity which is detrimental to grain growth.[9] Again, role of OH^- on boundary migration will depend on its location in the MgO lattice and any grain growth model derived from observed kinetics must be consistent with relevant microstructural features. As two distinct and apparently identical growth kinetics were observed at both 1300°C and 1500°C, the discussion here will be separated according to the two observed time dependencies. Grain growth data for OH^- doped MgO is given in Fig. 7.

(i) $t^{\frac{1}{2}}$ Dependence. ($t < 1000$ mins.)

Grain growth data for H120 at both 1300°C and 1500°C correspond to $n = 2$; a possible mechanism being boundary mobility control. However, presence of grain boundary porosity means pore control is more likely with volume diffusion as probable mechanism for their motion. Also, another indication of pore control is 1300°C data where two distinct growth rates are observed corresponding to specimens with different porosity content.

If OH^- does indeed go into solution creating Mg^{2+} lattice defects, then an approximate activation energy of 23 kcal/mol (2 data points) implies extrinsic Mg^{2+} diffusion as rate controlling. It has been speculated[8a] that surface adsorption of OH^-

enhances surface mobility of O^{2-} in predominantly ionic crystals so that cation migration would be rate controlling. Since grain boundaries are qualitatively similar to ceramic surfaces and if one assumes sufficient OH^- at grain boundaries (a reasonable assumption since one expects the hydroxide when added initially to MgO powder to be absorbed by the surface), a specific transport process for O^{2-} ion at MgO grain boundaries exist which makes Mg^{2+} diffusion as rate controlling a reasonable assumption.

(ii) $t^{\frac{1}{3}}$ Dependence. ($t > 2000$ mins.)

At 1300°C and 1500°C, data obeyed the kinetics law $D^3 = Kt$ suggesting porosity and/or impurity controlled growth. An additional temperature (1600°C) was studied and a cubic law was observed even at small heat treatments. No porosity or second phase inclusion were obvious but liquid phase wetting was evident at grain boundaries and triple points. These microstructural observation coupled with $t^{\frac{1}{3}}$ dependence indicate that at large grain size, material transfer across the grain boundary liquid phase is rate controlling. Liquid phase control is observed only at large anneal times (large grain size) because metal ions in Fisher MgO responsible for forming the eutectic phase takes awhile to diffuse to the grain boundary and secondly the grain boundary area must be low enough (large D) so that appreciable solid-liquid interfaces are formed. Appreciable liquid phase was observed even after 60 min. anneal at 1600°C because of the large grain size ($\sim 100 \mu m$).

The activation energy of 35 k cal/mol obtained for $t^{\frac{1}{3}}$ kinetics (Fig. 8) should correspond to diffusion through the liquid phase. As these activation energies are known to be extremely sensitive to composition of liquid phase any direct comparison with other liquid phase sintering data is not meaningful. However, the value seems reasonable and is close to value of 38 k cal/mole observed for densification in MgO in presence of LiF-rich grain boundary liquid phase.[36] Also, as there were regions in the microstructure where liquid phase wetting was observed strictly at the triple points (individual grains not surrounded by a liquid film), a possibility of boundary curvature

controlled solid-state grain growth also exists, the observed activation energy of 35 K cal/mole would then correspond to extrinsic lattice diffusion of the rate-controlling specie.

C. Comparison Between Anions

In the previous section grain growth in MgO in presence of each of the anions (F, S, Cl, OH) is discussed. It would be worthwhile now to compare and contrast the effect of these anions and determine how behavior in their presence differs from that of undoped MgO with respect to the actual grain growth rates (enhancement or inhibition) and the mechanism of pore migration and removal. The basis of such a comparison should be the location of these anions in the microstructure either as solid solution or as a second phase (gas, precipitate or a continuous liquid film).

For porous MgO (Figure 9), density gradients in hot pressed compacts (variations in translucency were routinely observed) give data scatter; as a result any local differences in grain sizes between different anions may not always be real. Hence, only general trends in grain growth behavior are meaningful and will be emphasized. The most striking observations in these figures is that there is very little difference in actual grain sizes at both 1300°C and 1500°C between anion doped and undoped Fisher MgO. Consequently, it appears that for less dense materials (> 1% porosity), kinetics are primarily pore controlled and effects of the anions, if any, are not very obvious. (Such porosity is difficult to avoid when these anions are present). Grain sizes for undoped material (UK130) at 1300°C (Fig. 9a) are closer to that for F material than for Cl or S (especially at low anneals) probably because of similarity in densities. In spite of differences in density between the different doped specimens, the limiting grain size at 1500°C (Fig. 9b) is the same (~ 65μ). Grain growth rate at (Fig. 9b) increases more rapidly at 1500°C but because of greater limiting effects it slows down and eventually becomes equivalent to that at 1300°C at long heat treatments (> 5000 mins.).

Influence of anions with respect to pore removal and boundary migration will be apparent only at very low porosity levels. For dense material (porosity < 1%), a very distinct difference in growth rates exists between OH^-, F^- and Cl^- (referred henceforth as promoters) as a group,

and S^{2-} which corresponds more to that of undoped Fisher MgO (Figure 11). As the densities of all these specimens (H120, F114, C115, S134 and UK132) are same, any difference in behavior should be interpreted as effect of the additive anions.

Larger grain sizes for "promoter" anions (OH^-, F^- and Cl^-) compared to S^{2-} can be interpreted as (1) lack of growth inhibition by inclusions (especially intergranular pores) which means the promoters aid densification, (2) mass diffusion rates are higher. OH^- and F^- are known to enhance matter diffusion by creating excess lattice defects on substitution for O^{2-} and under certain conditions form grain boundary liquid phase. On the other hand, the mechanism for Cl (also applicable for F) is proposed to be pore transport with the grain boundary by evaporation - condensation process normally important only at high temperatures in MgO. At sintering temperature, the gas phase (probably Cl_2) inside the pores is in equilibrium with solid MgO in such a way that on the pore surface with lesser curvature (less concave) volatile compounds (oxychloride) are continuously forming, move by vapor transport to the more concave pore surface, and there are continuously dissociating back into the oxide and Cl_2, the overall process resulting in pore motion. Similar mechanism was proposed by Eudier[37] for activated sintering of Cu by oxygen (confirmed latter by experiments[38]) and iron in presence of hydrogen halides. Bockstiegel[39] has reported such facilitation of gas phase transport by action of even sulphur on iron. However, no such enhancement of pore migration was evident in grain growth studies of sulphur doped magnesia.

Considering first, the 1300°C data (Fig.10a), the promoters are equivalent within the scatter limits, especially at large anneal times (could be fortitious in view of different mechanisms possible). However, the reason is not immediately obvious for high grain sizes for OH^- specimens compared to F^- (in view of identical mechanisms) at $t < 400$ mins.

Again, occurrence of a limiting grain growth for all three anions at about the same grain size (200μ m) is surprising in view of greater porosity observed for the Cl^- specimen . On the other hand, possibility of limiting growth due to specimen size (surface effect) must be considered. Identical time dependence and growth rates for S^{2-} specimen (S134) and undoped Fisher MgO (UK132) could mean two things; either sulphur has no appreciable effect on microstructure and hence, no effect on boundary migration rate or, insufficient S^{2-} was retained in the material after hot-pressing to give observable effect. (Note that as pressed analysis of sulphur doped specimens (Table III) do indeed indicate that S has been lost during hot-pressing).

The above observations are generally true even at 1500°C for dense compacts. Fig. 11b / S behaves differently from OH^-, F^- and Cl^-, in fact data for S^{2-} corresponds closely with that for Fisher MgO (HP332 and UK132) both in growth rates and presence of constant grain size plateau (70μ). An obvious effect of F^- is absence of such a plateau (rapid densification) while OH^- shows limiting growth only at large grain size and for a very short time. Again, the grain sizes for OH^- are larger than for F^- at low anneals, however, they become equivalent at large anneals. Hence, on comparison, the effect of these anions on grain growth is in the order $OH^- > F^- > Cl^- > S^{2-} \approx$ (Undoped Fisher MgO). Anion impurities were shown[9] to be deleterious to densification of MgO by hot pressing in the order $S^{2-} > Cl^- > F^- > OH^-$. Hence, any effect of these anions on grain growth can be related directly to their effect on densification.

Lastly, OH^-, F^- and Cl^- give vastly different grain sizes for different porosity levels while S^{2-} behaves more like undoped material where growth rates are insensitive to density differences.

V. Summary and Conclusions

(1) Porosity is an essential microstructural feature of hot-pressed powder compacts; in very pure material, porosity controls grain growth even when present in very small quantities (< 1/2%). However, most anion additives have a definite effect on pore mobility and densification and hence their presence reduces pore inhibition and gives impurity controlled boundary migration at large grain sizes.

(2) Effects of anion additives are important only when porosity level in MgO material is sufficiently low (< 1%); when material is porous (> 1% porosity), boundary migration is predominantly pore controlled.

(3) OH^-, F^- and Cl^- gave higher grain growth rates than Fisher MgO and hence they are growth promoters. In present work, S^{2-} showed no effect. In fact, effect on growth rates is in the order $OH^- > F^- > Cl^- > S^{2-}$, the effectiveness depends on the form in which they exist in the mictostructure.

(4) Grain sizes in undoped and S^{2-} doped MgO were insensitive to vast differences in specimen density while definite dependence of growth rate on density was observed in presence of OH^-, F^- and Cl^-.

(5) The above conclusions are general. However, the kinetics observed may not always be representative of a particular anion but could change with different porosity and impurity distribution in a given specimen. Hence, any model about rate controlling mechanisms from observed kinetics alone is of little value unless supported by microstructural observations.

References

1. M. H. Leipold, J. Amer. Ceram. Soc., 49 [9] 498-502 (1966).
2. V. S. Stubican and D. Viechnicki, J. Appl. Phys., 37 [7] 2751 (1966).
3a. G. C. Nicholson, J. Am. Ceram. Soc. 48 [10] 525-528 (1965).
3b. G. C. Nicholson, J. Am. Ceram. Soc. 49 [1] 47-49 (1966).
3c. I. Amato, R. L. Colombo, A. Petruccioli Balzari, J. Nucl. Mater. 18 [3] 252-260 (1966).
3d. R. S. Gordon, D. D. Marchant, and G. W. Hollenberg, J. Am. Ceram. Soc., 53 [7] 399-406 (1970).
4. R. Rice, Ultra Fine Grain Ceramics, Syracuse Univ. Press, Syracuse, N. Y., p. 203 (1970).
5. T. H. Nielsen and M. H. Leipold, J. Am. Ceram. Soc., 49 [11] 626 (1967).
6. F. Freund, J. Am. Ceram. Soc., 50 [9] 493 (1967).
7. A. J. Socha and M. H. Leipold, J. Am. Ceram. Soc., 48 [9] 463 (1965).
8a. P. J. Anderson and P. L. Morgan, Trans. Farad. Soc., 60 [5] 930-937 (1964).
8b. J. White, High Temperature Oxides - Part I, Academic Press, New York, p. 80 (1970).
8c. R. M. Dell and S. W. Weller, Trans. Faraday Soc., 55 [12] 2203-2220 (1959).
9. M. H. Leipold and C. M. Kapadia, J. Am. Ceram. Soc., 56 [4] 200-203 (1973).
10. David Turnbull, Trans. A.I.M.E. 191 [8] 661-665 (1951).
11. G. F. Bolling and W. C. Winegard, Acta Met., 6 [4] 283-287 (1958).
12. R. M. Spriggs, L. A. Brissette and T. Vasilos, J. Amer. Ceram. Soc., 47 [8] 417-418 (1964).
13. F. A. Nichols, J. Am. Ceram. Soc., 51 [8] 468-469 (1968).
14. P. G. Shewmon, Trans. A.I.M.E., 230 [5] 1134-1137 (1964).
15. A. Mocellin and W. D. Kingery, J. Am. Ceram. Soc., 56 [6] 309-314 (1973).

16. R. J. Brook, J. Amer. Ceram. Soc., 52 [6] 339-340 (1969).

17. W. V. Speight, Acta Met. 16 [1] 133-35 (1968).

18. K. W. Lay, J. Amer. Ceram. Soc., 51 [7] 373-376 (1968).

19. W. D. Kingery and B. Francois, J. Am. Ceram. Soc., 48 [10] 546-547 (1965).

20. C. M. Kapadia, Ph.D. Thesis. To be published.

21. P. G. Shewmon, Transformation in Metals, Chapt. 3, McGraw-Hill Book Co., New York, 1969.

22. N. A. Haroun and D. W. Budworth, J. Mater. Sci., 3 [3] 326-328 (1968).

23. M. H. Leipold and T. H. Nielsen, Am. Ceram. Soc. Bull. 45 [3] 281-285 (1966).

24. M. H. Leipold and C. M. Kapadia, Tech. Rept. UKY 25-70-Met-12, June 1970.

25. J. E. Hilliard, "Grain Size Estimation," General Electric Research Rept. No. 61-RI-2898M, 1961.

26a. G. D. Miles, R. A. J. Sambell, J. Rutherford and G. W. Stephenson, Trans. Brit. Ceram. Soc., 66 [7] 319-335 (1967).

26b. Edward Carnall, Jr., Mater. Res. Bull., 2 [12] 1075-1086 (1967).

26c. S. G. Carniglia, R. E. Johnson, A. C. Hott and G. G. Bentle, J. Nucl. Mater. 14, 378-394 (1964).

27. Rinoud Hanna, Amer. Ceram. Soc. Bull., 49 [5] 548-549 (1970).

28. J. Gittins and O. F. Tuttle, Am. J. Sci. 262, 66-75 (1964).

29a. R. Rice, J. Amer. Ceram. Soc. 54 [4] 205-207 (1971).

29b. R. K. Stringer, C. E. Warble, and L. S. Williams, Kinetics of Reactions in Ionic Systems, Chapter 4, Plenum Press, New York (1969).

30. M. W. Benecki, N. E. Olson, and J. A. Pask, J. Am. Ceram. Soc. 50 [7] 365-368 (1967).

31. E. J. Felten, J. Amer. Ceram. Soc. 44 [6] 251-255 (1961).

32. F. A. Nichols, J. Appl. Phys. 37 [13] 4599-4602 (1966).

33. H. Schäfer, Chemical Transport Reactions, Chapter 3, Academic Press, New York 1964.

34. Paul F. Eastman and Ivan B. Cutler, J. Amer. Ceram. Soc., 49 [10] 526-530 (1966).

35. P. J. Wyllie, J. Amer. Ceram. Soc., 50 [1]43-46 (1967).

36. P. E. Hart, R. B. Atkin, and J. A. Pask, J. Amer. Ceram. Soc., 53 [2]83-86 (1970).

37. A. J. Shaler, Sintering and Related Phenomena, Gordon and Breach, New York 1965, p. 807.

38. T. P. Hoar and J. M. Butler, Jour. Inst. of Met., 78, 351 (1950).

39. G. Bockstiegel, Powder Metallurgy, 10, 171, 1962.

LIST OF FIGURES

Table I

Factors Controlling Grain Boundary Mobility

Controlling Factors		
1. Boundary Mobility (Normal growth)	2. Pore Mobility (Normal growth)	3. Both (Discontinuous growth)
Relative magnitudes of mobilities		
a) $\frac{M_p}{N} >> M_b$	$\frac{M_p}{N} << M_b$	$M_b >> M_p (\approx 0)$
Boundary velocity equation		
b) $V = M_b F_b$	$V = \frac{M_p F_b}{N}$ (N = number of pores)	$V = M_b F_b$ for those grains grains whose diameter is much larger than the matrix grain diameter.
c) Boundary mobility controls (n = 2)	Pore mobility controls (n > 2)	Mixed control
Conditions when behavior is present		
d) Low temperature, therefore, M_b is small	High temperature (anneal time could be small), therefore M_b is large	High temperature
e) Low anneal time and small grain size, therefore r_p is small and M_p is large	Large anneal time (Temperature could be low) and large grain size, therefore r_p is large and M_p is small	

Table II

Values of m for Different Pore Transport Mechanisms and Corresponding Grain Growth Exponents (n)

Mechanism	m	n		Conditions when applicable		
		$n = m$ † (pores at boundary intersection)	$n = m - 1$ * (pores on individual grain boundaries)	Pore radius r_p	Temperature	Vapor Pressure
Surface diffusion	4	4	3	small	low	low
Volume diffusion	3	3	2	Intermediate	Intermediate	low
Vapor transport (p = constant)	3	3	2	Large ($\geq 1\mu$)	high	high
Vapor transport $\left(p = \frac{2\gamma_{sv}}{r_p}\right)$	2	2	1	Large ($\geq 1\mu$)	high	high

TABLE III

Composition and Fabrication Parameters for Specimens Used for Grain Growth Studies

Specimen	Dopant	Hot Pressing Conditions			As pressed density g/cm³	As pressed analysis At%
		Max. Temp. °C	Max. Press. KSI	Atmos*		
			UNDOPED MgO			
OP 356	None	1025	13	V	3.58 (100%)	
OP 373	None	1050	13	V	3.55 (99.4%)	
HP 332‡	None	1270	4	A†	3.56 (99.6%)	
UK 132	None	1000	15	A	3.56 (99.6%)	
UK 130	None	1000	15	A	3.52 (98.4%)	
			DOPED MgO			
H 120	3% OH	1100	15	V	3.54 (98.8%)	
H 74	3% OH	1050	15	A	3.41 (95.5%)	
F 114	3% F	1100	15	V	3.56 (99.6%)	0.68
F 110	3% F	1100	15	V	3.53 (98.7%)	0.90
C 48	3% Cl	1170	17	V	3.42 (95.6%)	NAξ
C 115	3% Cl	1100	15	V	3.56 (99.6%)	0.06
S 33	1% S	960	20	V	3.43 (95.8%)	0.24
S 96	3% S	1100	15	V	3.49 (97.6%)	0.31
S 134	6% S	1000	15	A	3.55 (99.3%)	0.04

* A = Argon; V = Mechanical pump vacuum

ξ NA = as pressed analysis not available

† carbonaceous Argon

‡ die assembly was of graphite, for all others it was of Al_2O_3.

TABLE IV

Physical Properties of Anion Impurities

Specie	Diameter Å	Diameter %Diff. from O^{2-}	Vapor Pressure @ 1000°C (atm)‡ Element	Vapor Pressure @ 1000°C (atm)‡ MgX_n
O^{2-}	2.80	0	$> 10^3$	$< 10^{-6}$
OH^-	2.76	-1.4	$\sim 10^3$	15
OD^-	2.76	-1.4	$\sim 10^3$	15
F^-	2.72	-2.9	$> 10^4$	$< 10^{-6}$
Cl^-	3.62	+29.2	$> 10^3$	0.3
S^{2-}*	3.68	+31.4	15	$< 10^{-6}$

‡Data from Handbook of Physics and Chemistry and use of Duhring's Rule when necessary.

*In sulphur doped specimens, the formation of SO_2 or SO_3 would result in a high vapor pressure which promotes residual porosity.

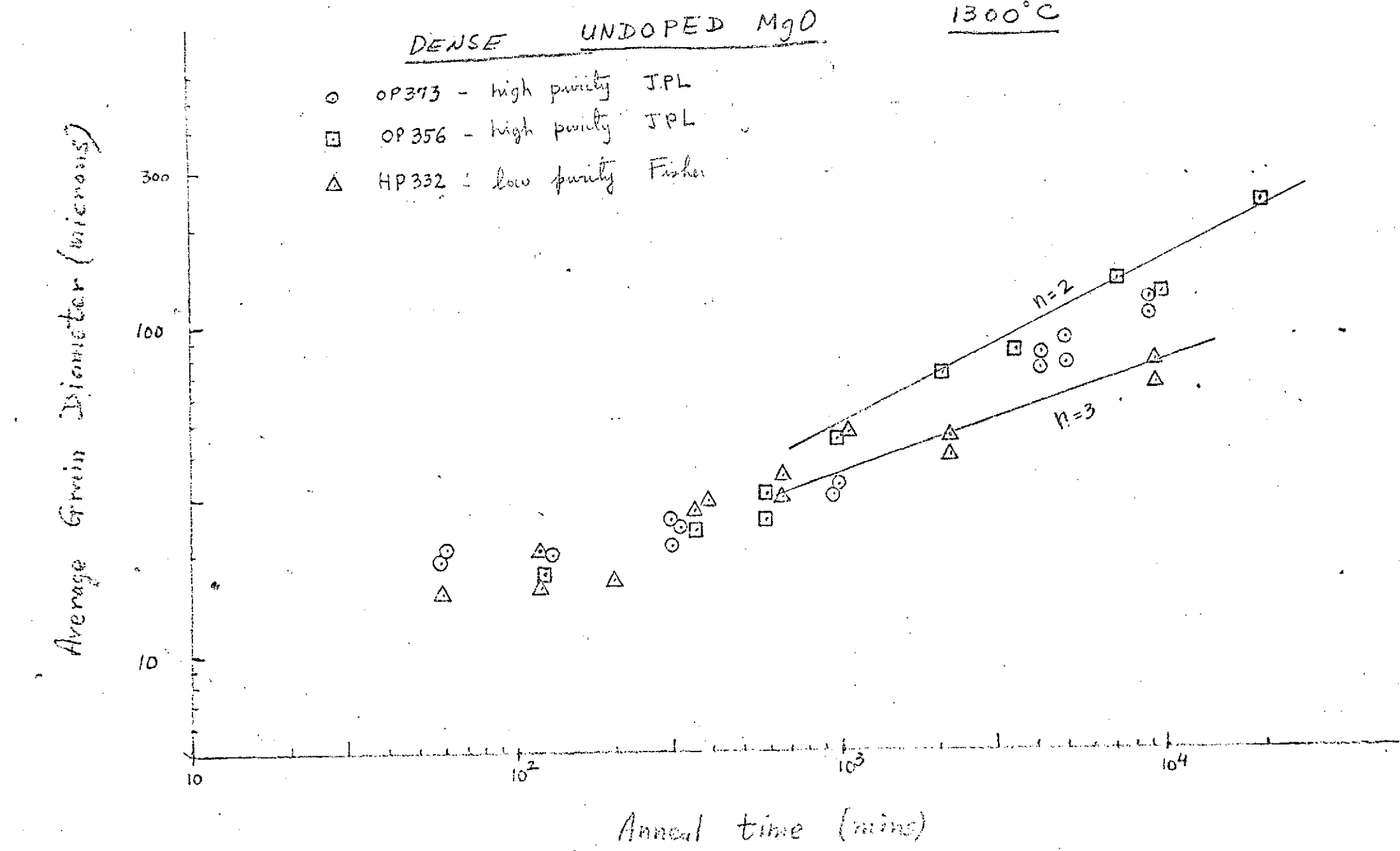
DENSE UNDOPED MgO
1300°C
OP373 - high purity JPL
OP356 - high purity JPL
HP332 - low purity Fisher
n=2
n=3
Average Grain Diameter (microns)
300
100
10
10
10²
10³
10⁴
Anneal time (min)

Figure 1(a)

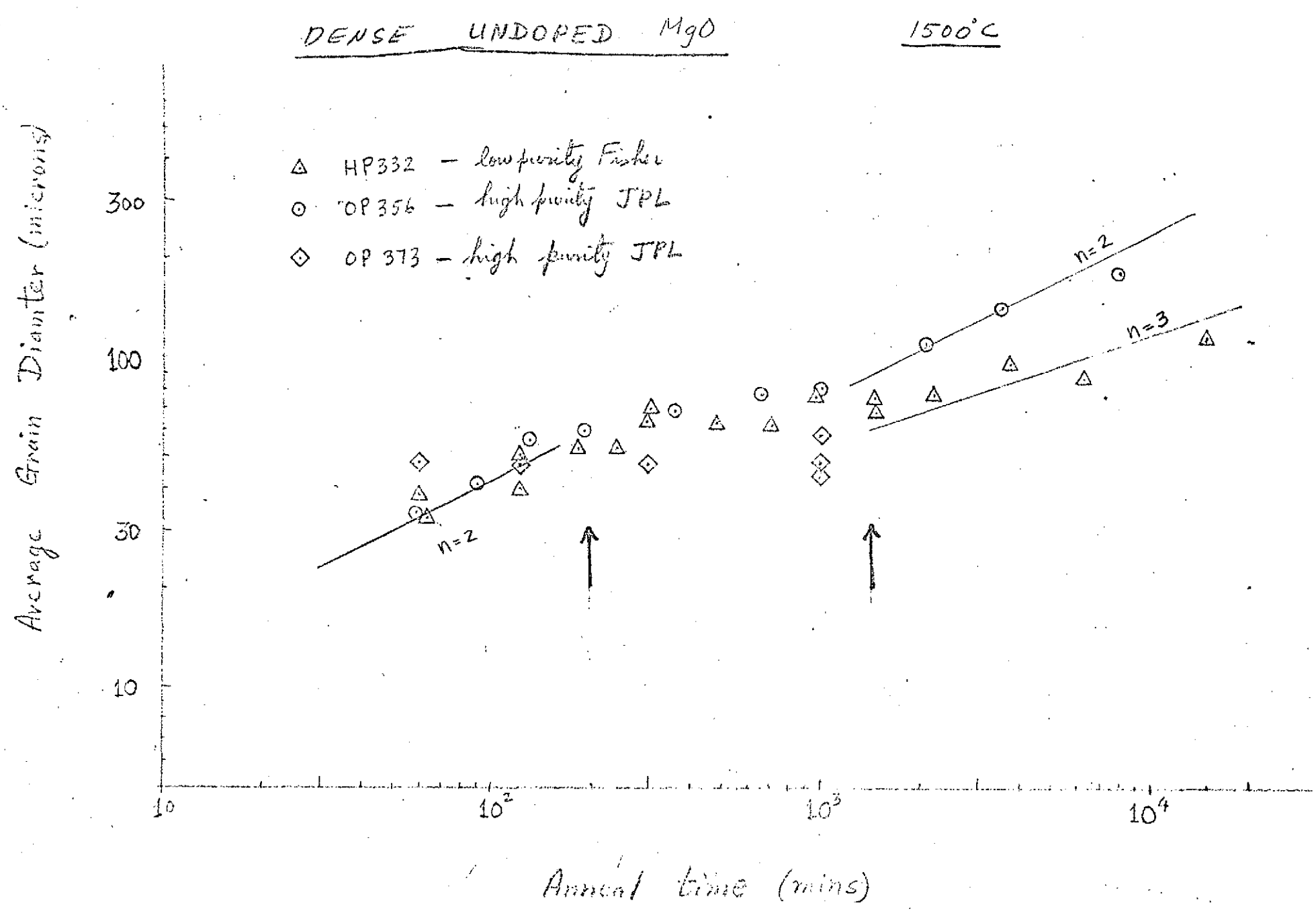
DENSE UNDOPED MgO
1500°C
HP332 – low purity Fisher
OP356 – high purity JPL
OP373 – high purity JPL
n=2
n=3
n=2
Average Grain Diameter (microns)
300
100
30
10
10
10²
10³
10⁴
Anneal time (mins)

Figure 1(b)

UNDOPED FISHER MgO 1300°C

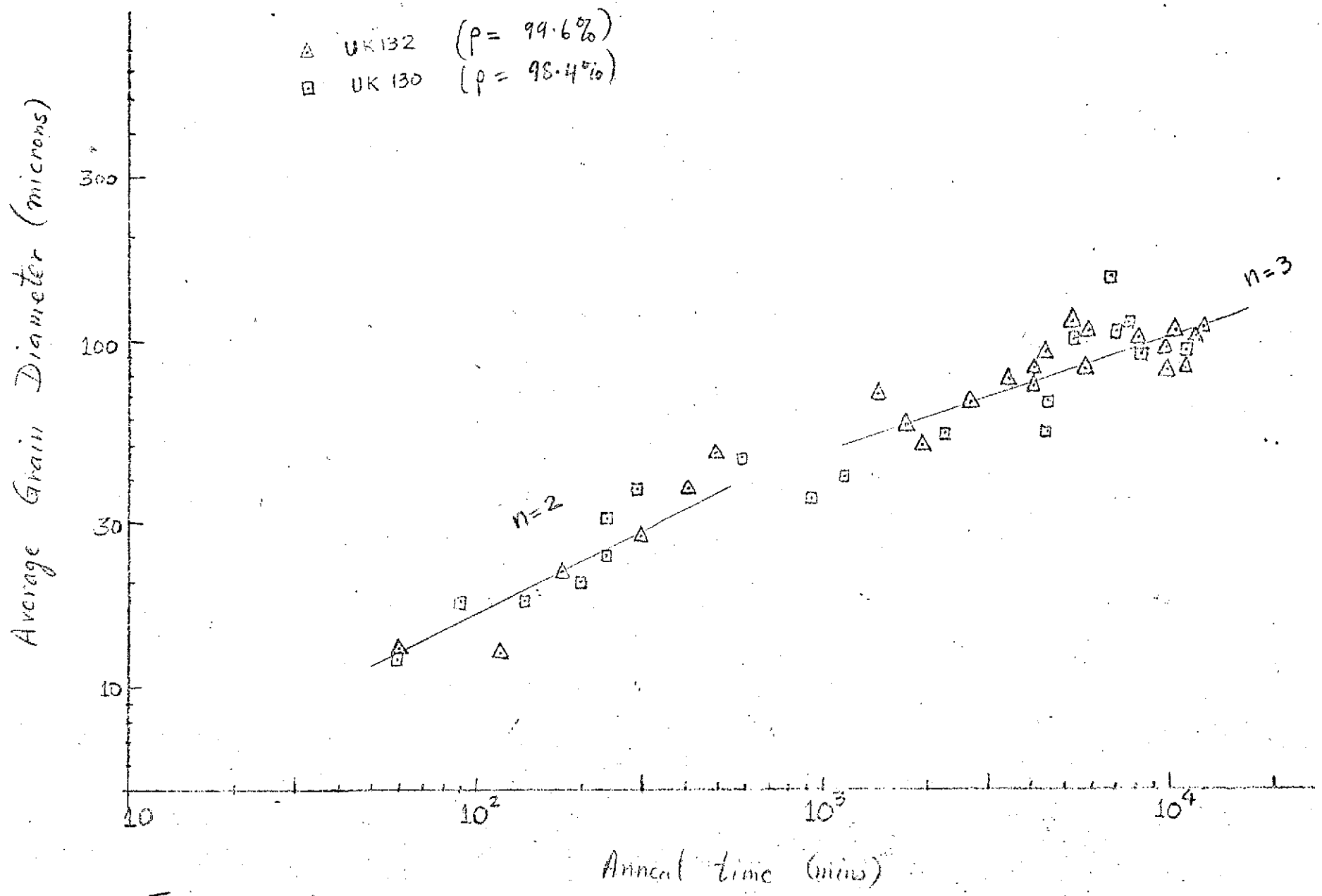

Figure 2(a)

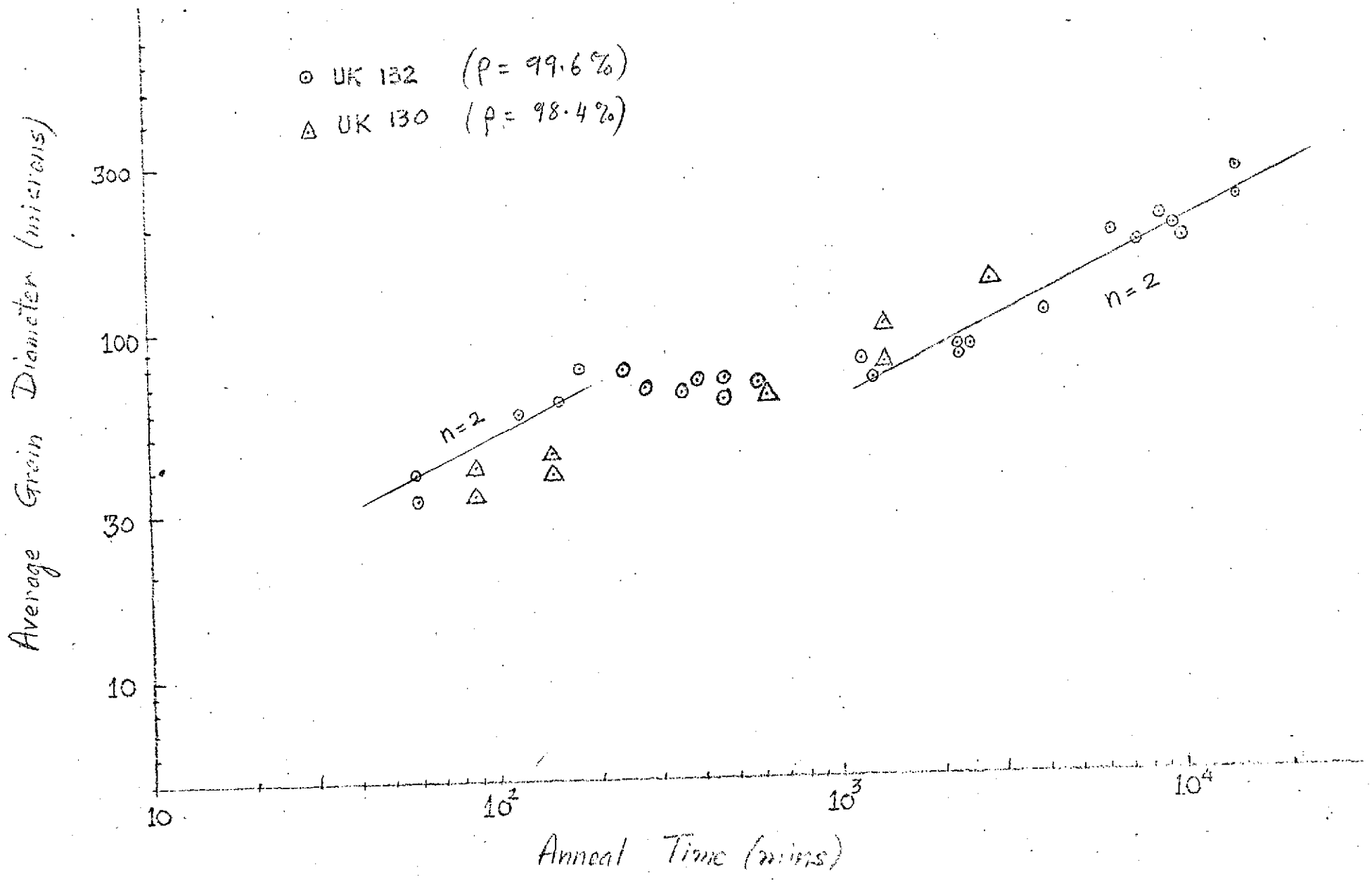
UNDOPED FISHER MgO 1500°C
UK 132 (ρ = 99.6%)
UK 130 (ρ = 98.4%)
n=2
n=2
300
100
30
10
10
10²
10³
10⁴
Average Grain Diameter (microns)
Anneal Time (mins)

Fig 2(b)

Fluorine doped Fisher MgO 1300°C

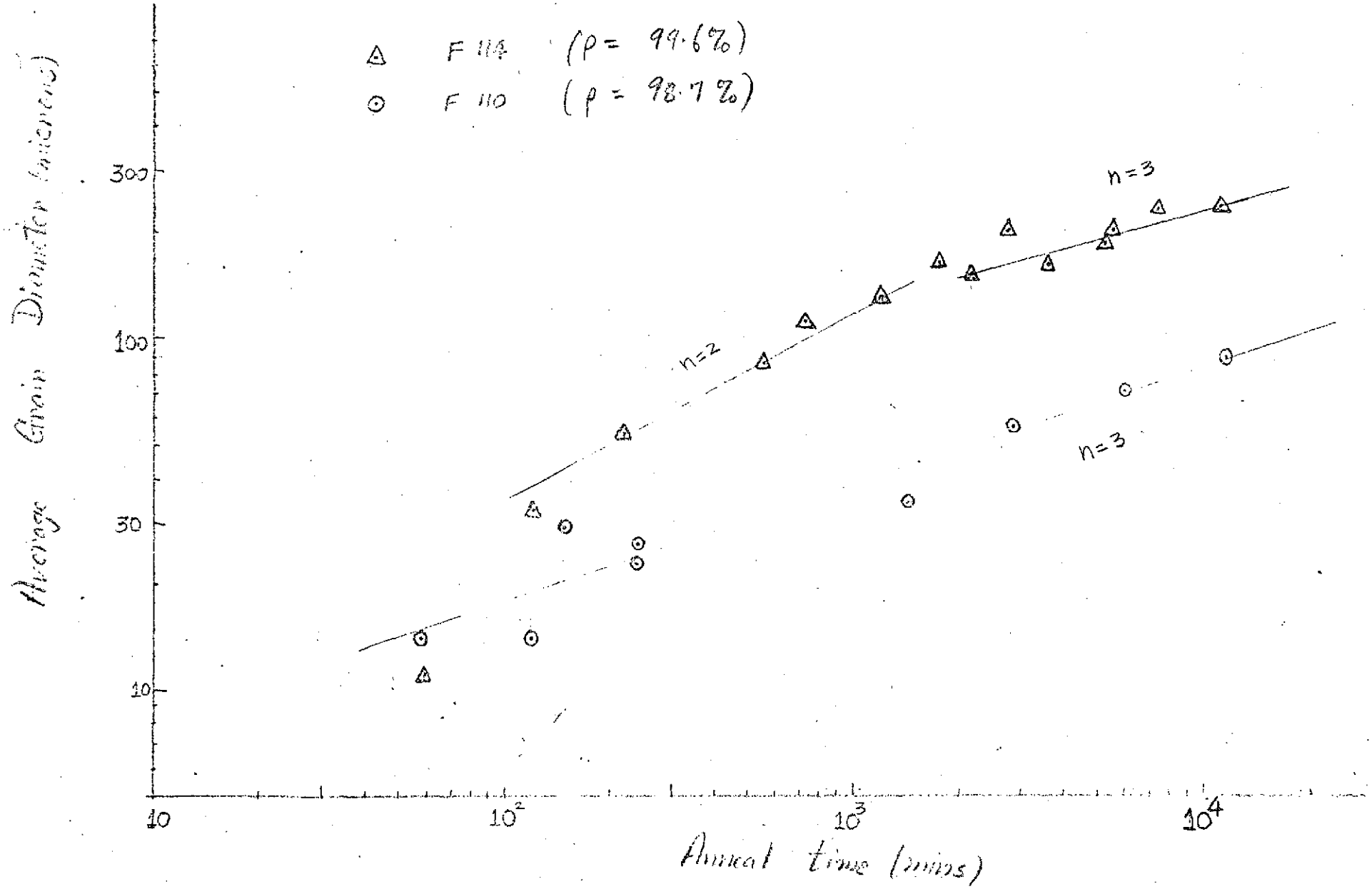

Fig 3(a).

Fluorine doped Fisher MgO 1500°C

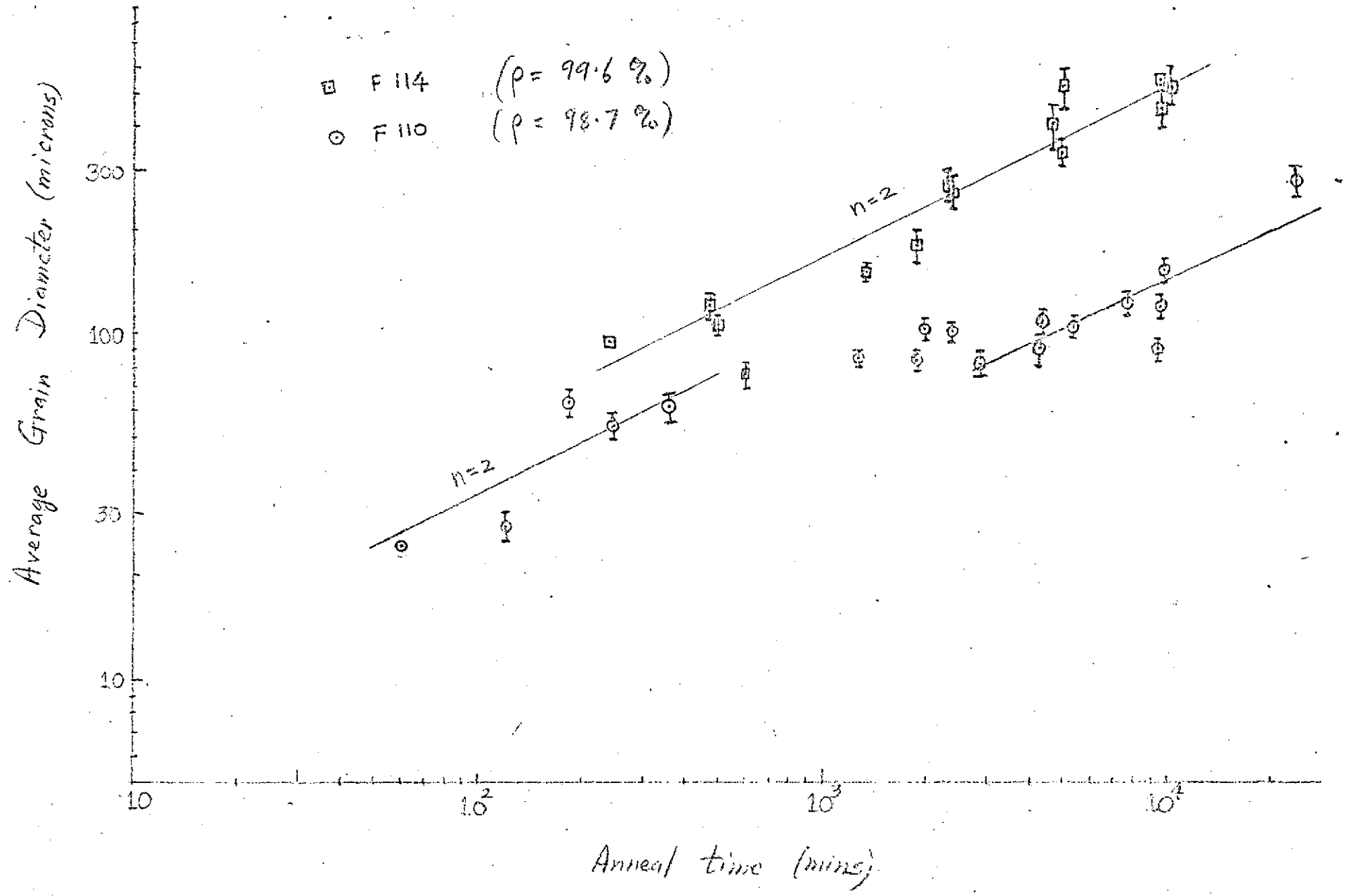

Figure 3(b)

Chlorine doped Fisher MgO 1500°C

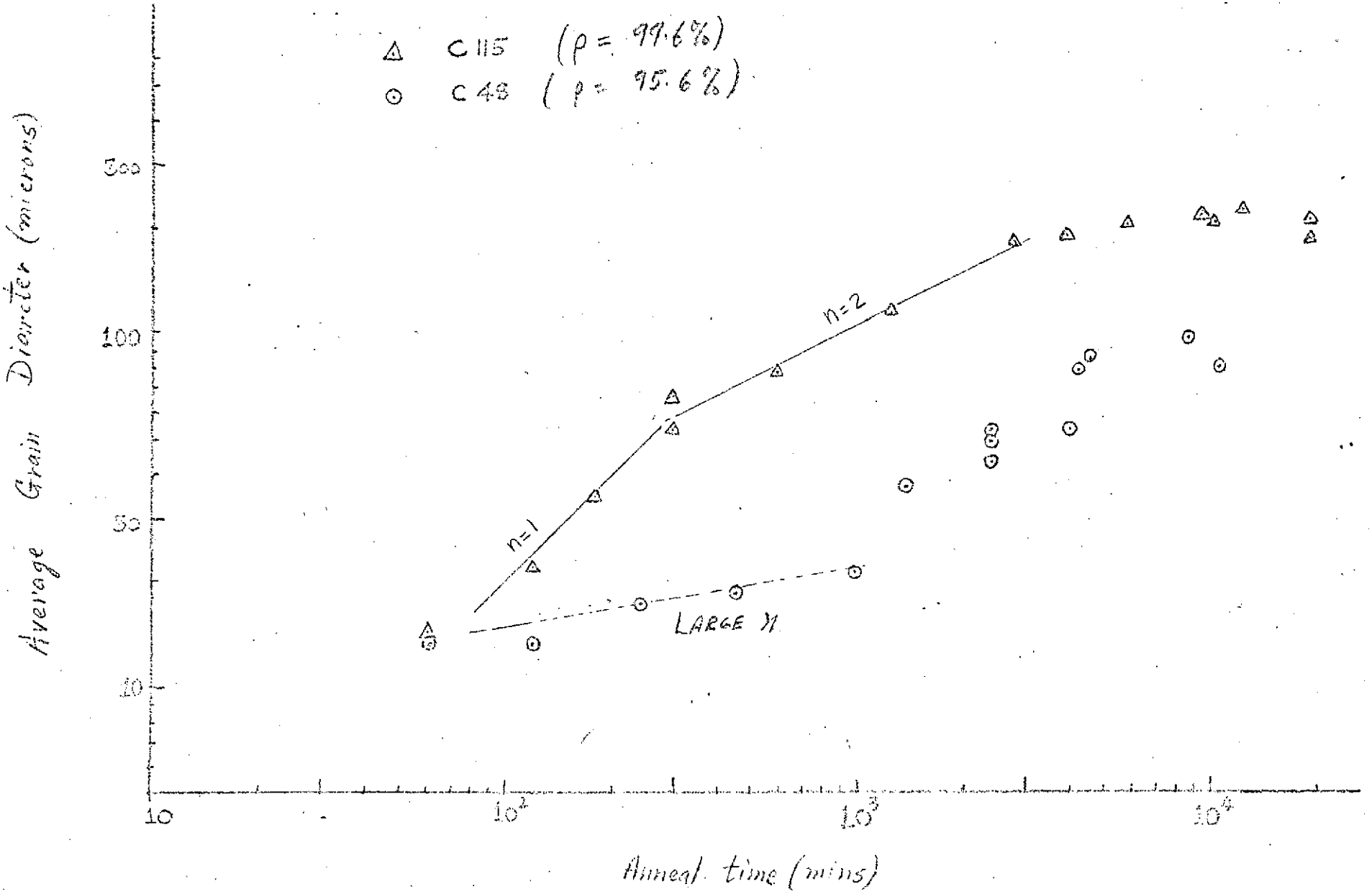

Figure 4(a)

Chlorine doped Fisher MgO 1500°C

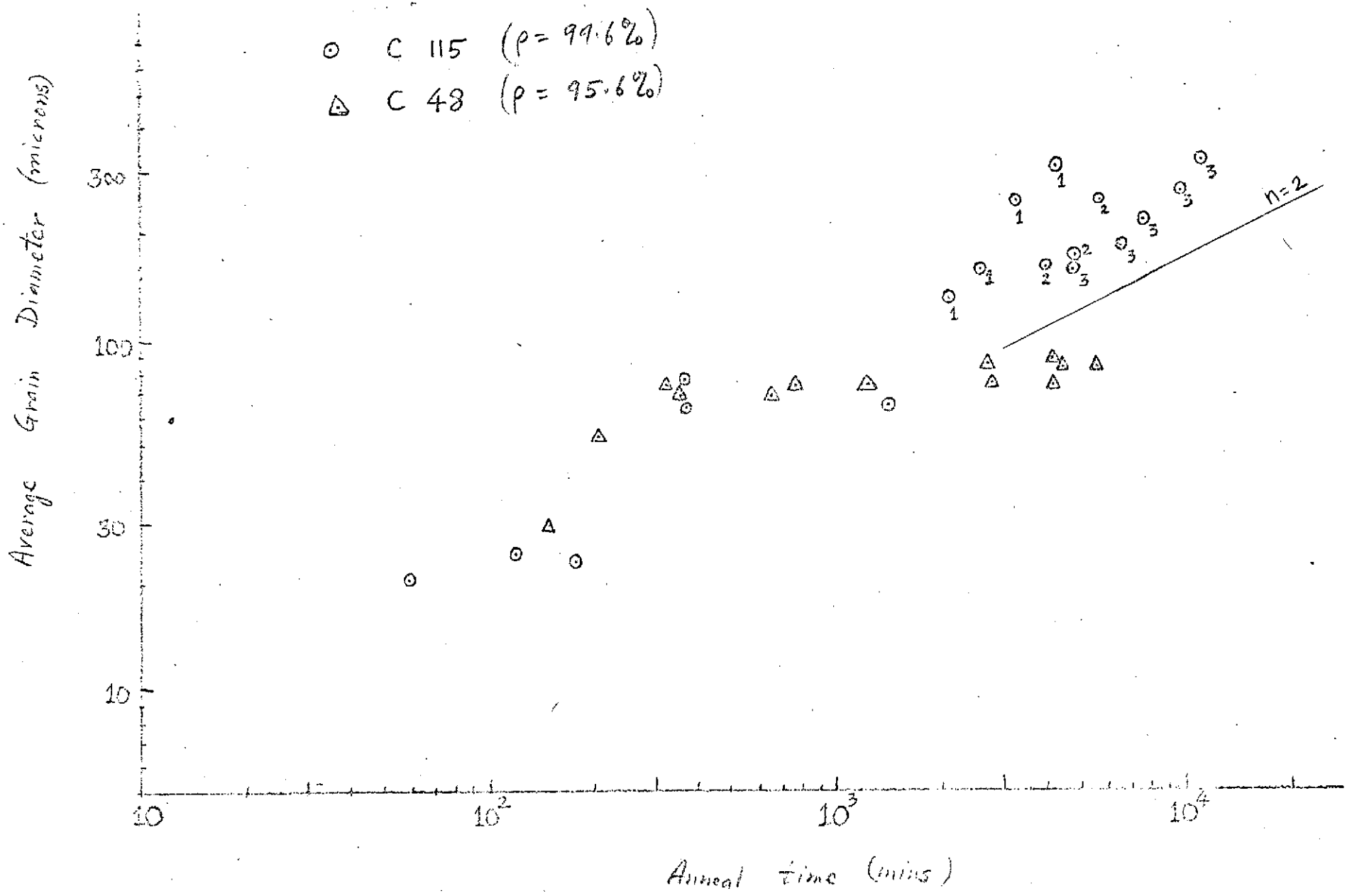

Figure 4 (b)

Sulphur doped Fisher MgO 1300°C

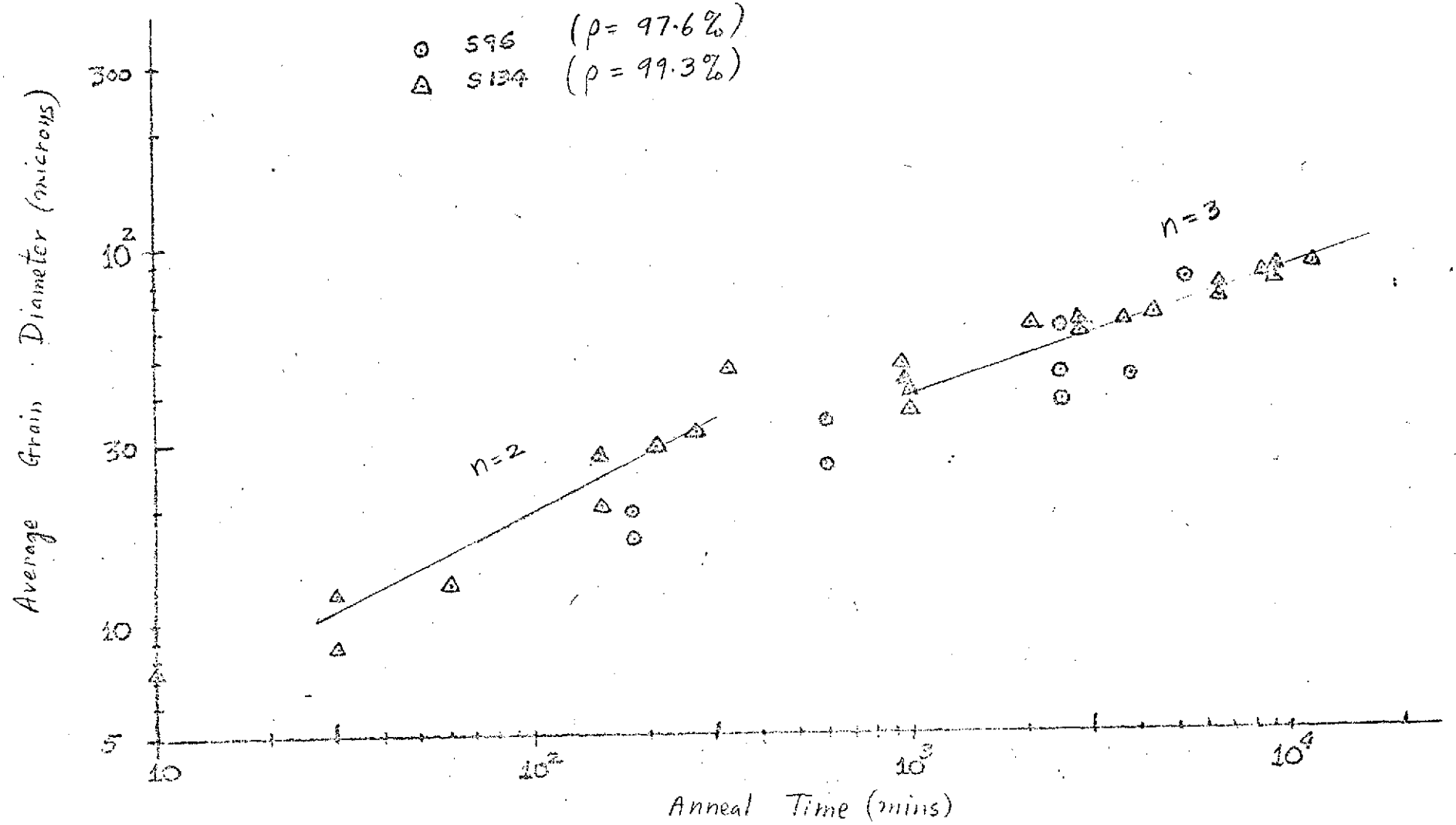

Figure: 5(a)

1300

Sulphur doped Fisher MgO 1500°C

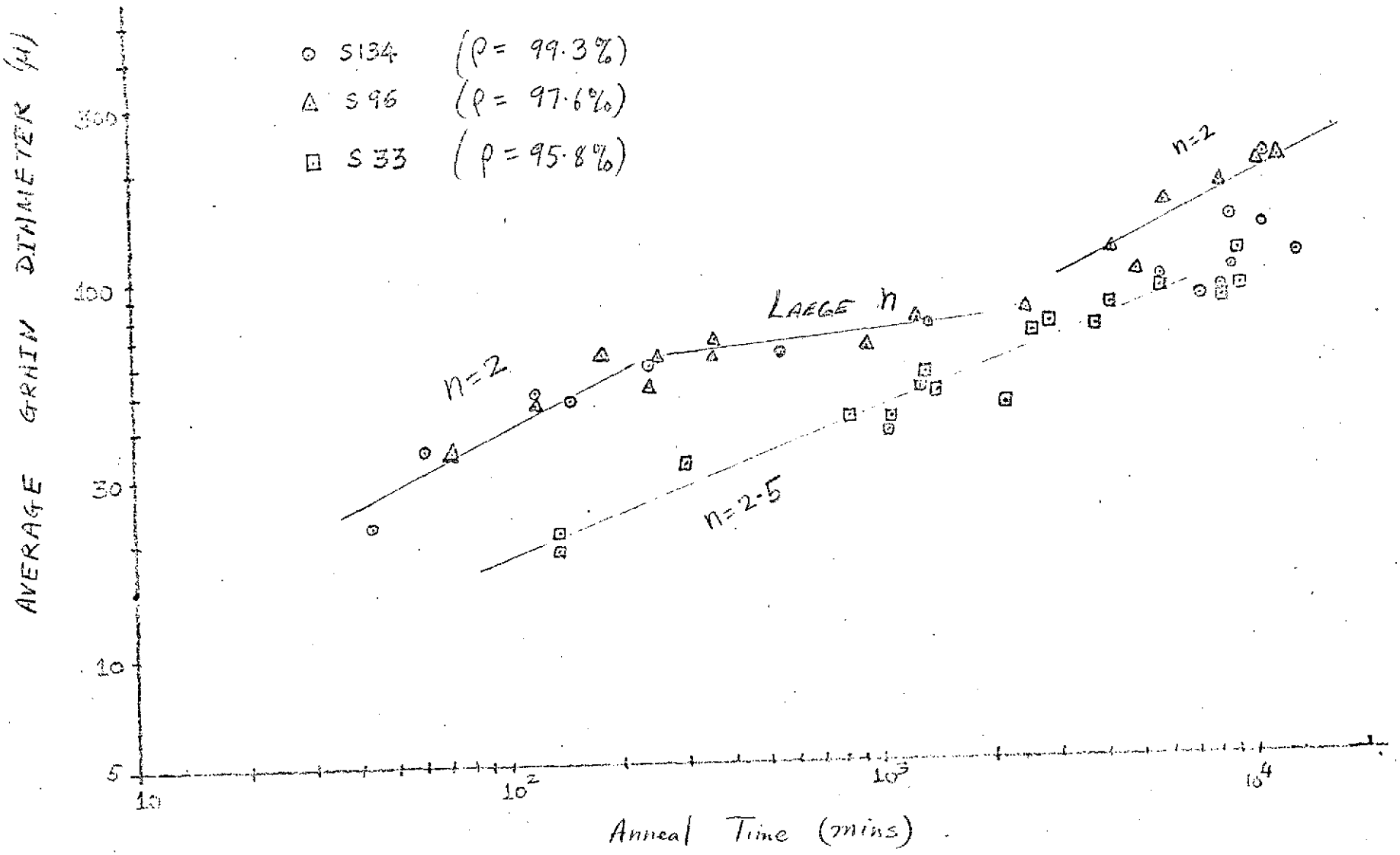

Figure 5(b)

Fig. 6a. Scanning electron micrograph (BSE) of 1.08% sulphur doped MgO (reheated for 48 hours at 1500°C) Polished and etched. Arrow shows possible $CaSiO_3$ phase at triple point.

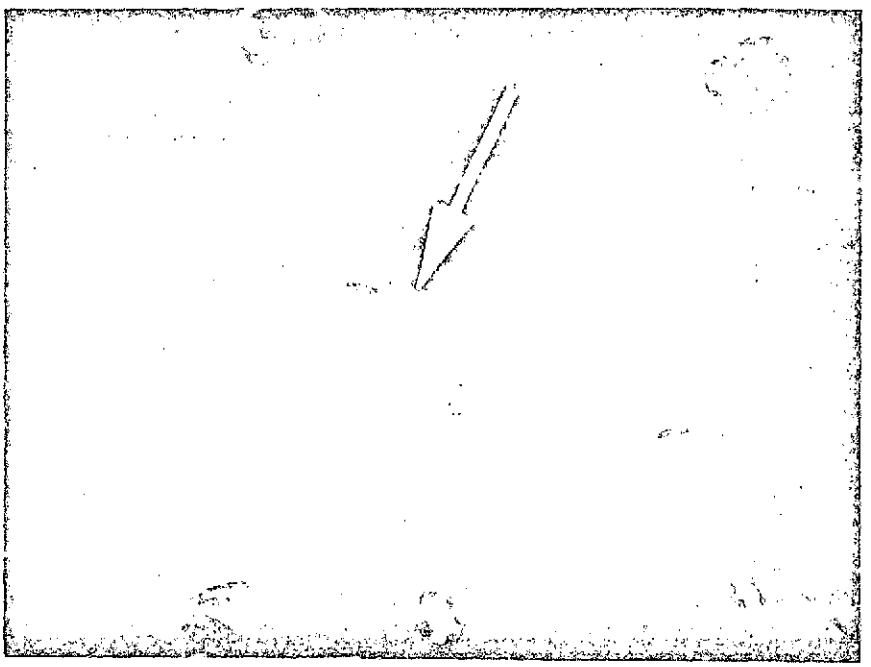

Fig. 6b. Same region as above at higher magnification indicating possible existence of second phase particles in the pore-like inclusions. Arrow (black) shows a tiny pore within one of these particles.

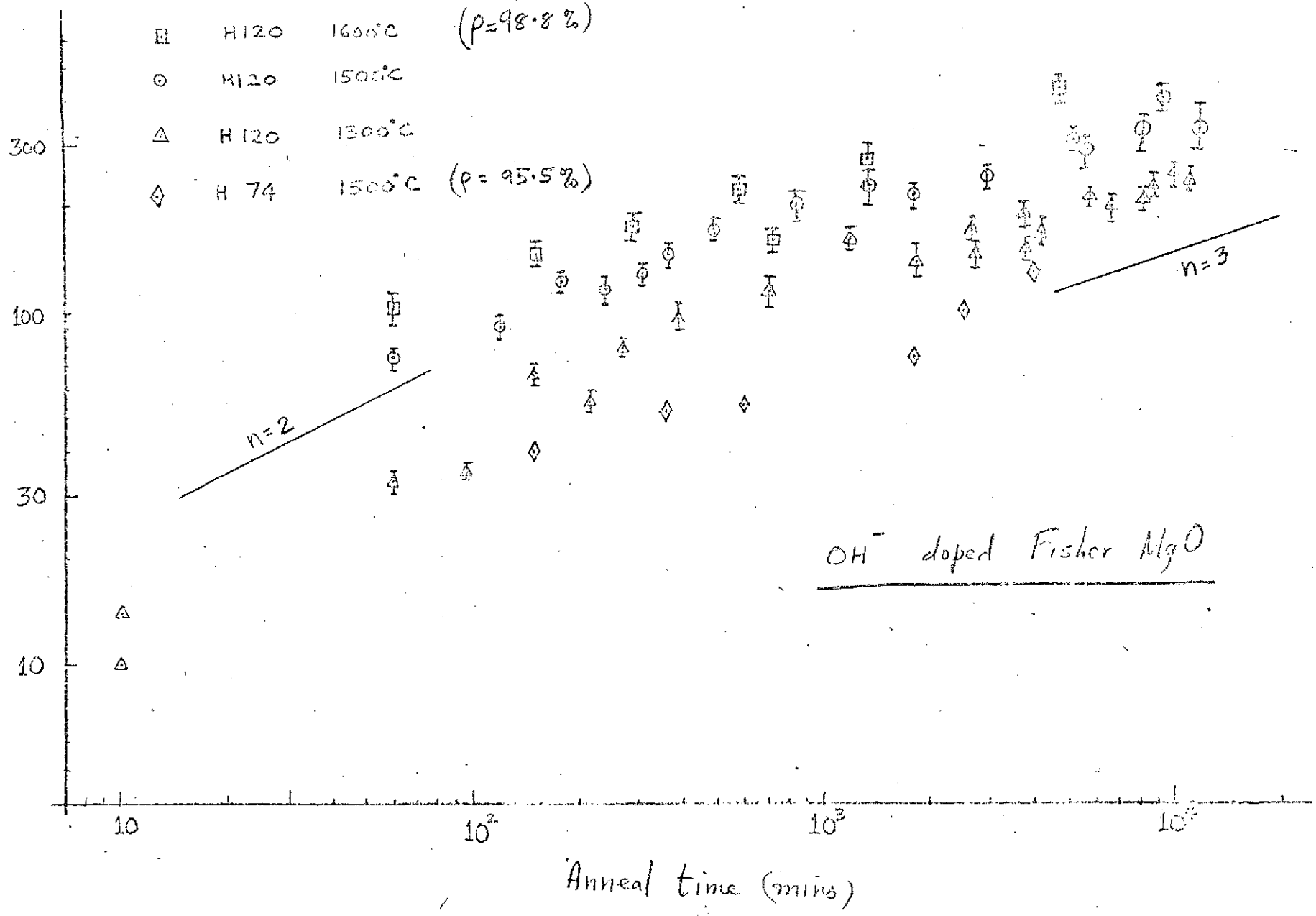

Figure 7

Std 21

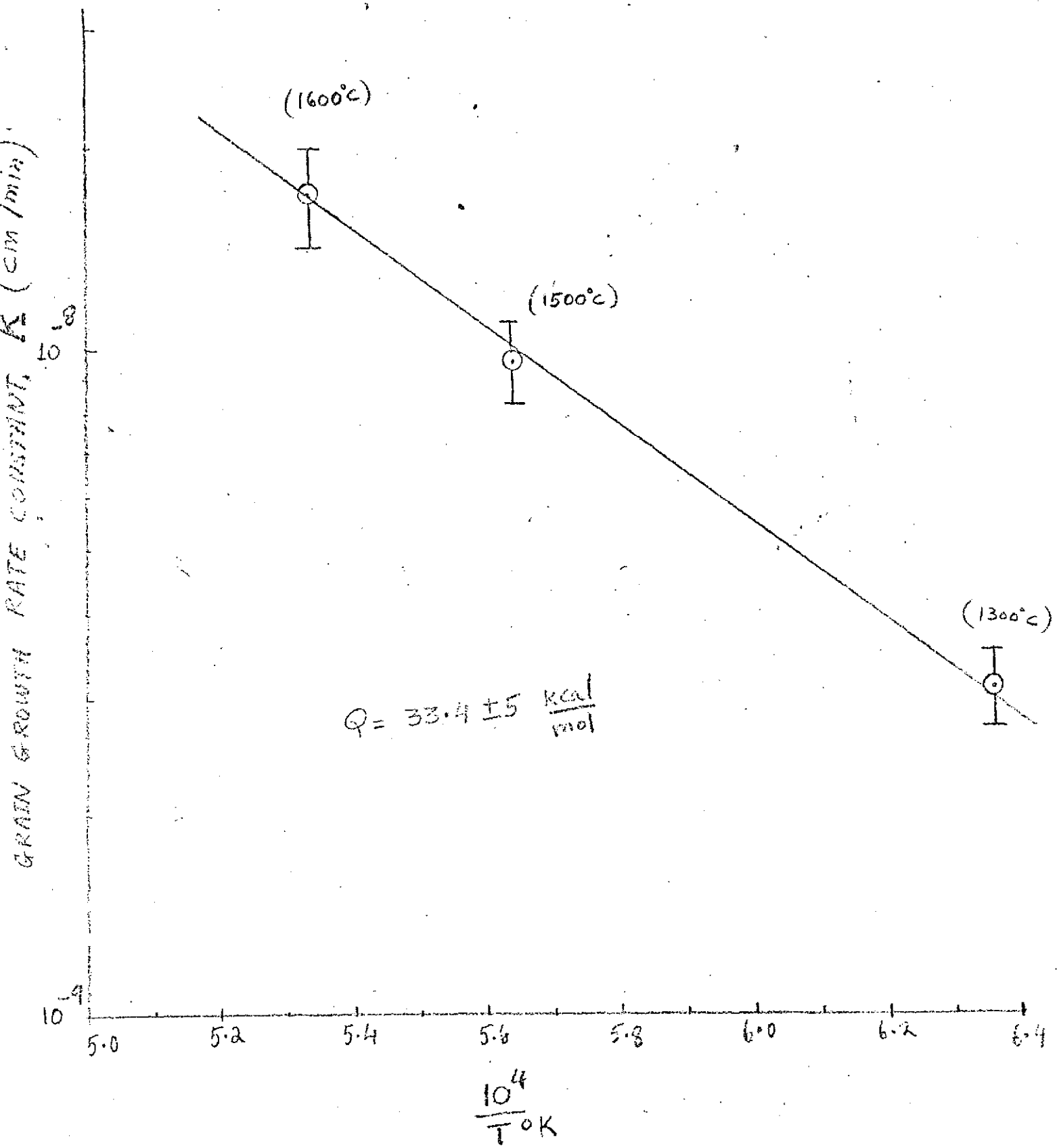
GRAIN GROWTH RATE CONSTANT, K (cm³/min)
10⁻⁸
10⁻⁹
(1600°C)
(1500°C)
(1300°C)
Q = 33.4 ± 5 kcal/mol
5.0
5.2
5.4
5.6
5.8
6.0
6.2
6.4
10⁴/T °K

Figure 8

ANION DOPED FISHER MgO (1–4% POROSITY)

1300°C

			DOPANT
⊡	UK 130	(ρ = 98.4%)	UNDOPED
⊙	S 96	(ρ = 97.6%)	S
△	C 48	(ρ = 95.6%)	Cl
—	F 110	(ρ = 98.7%)	F

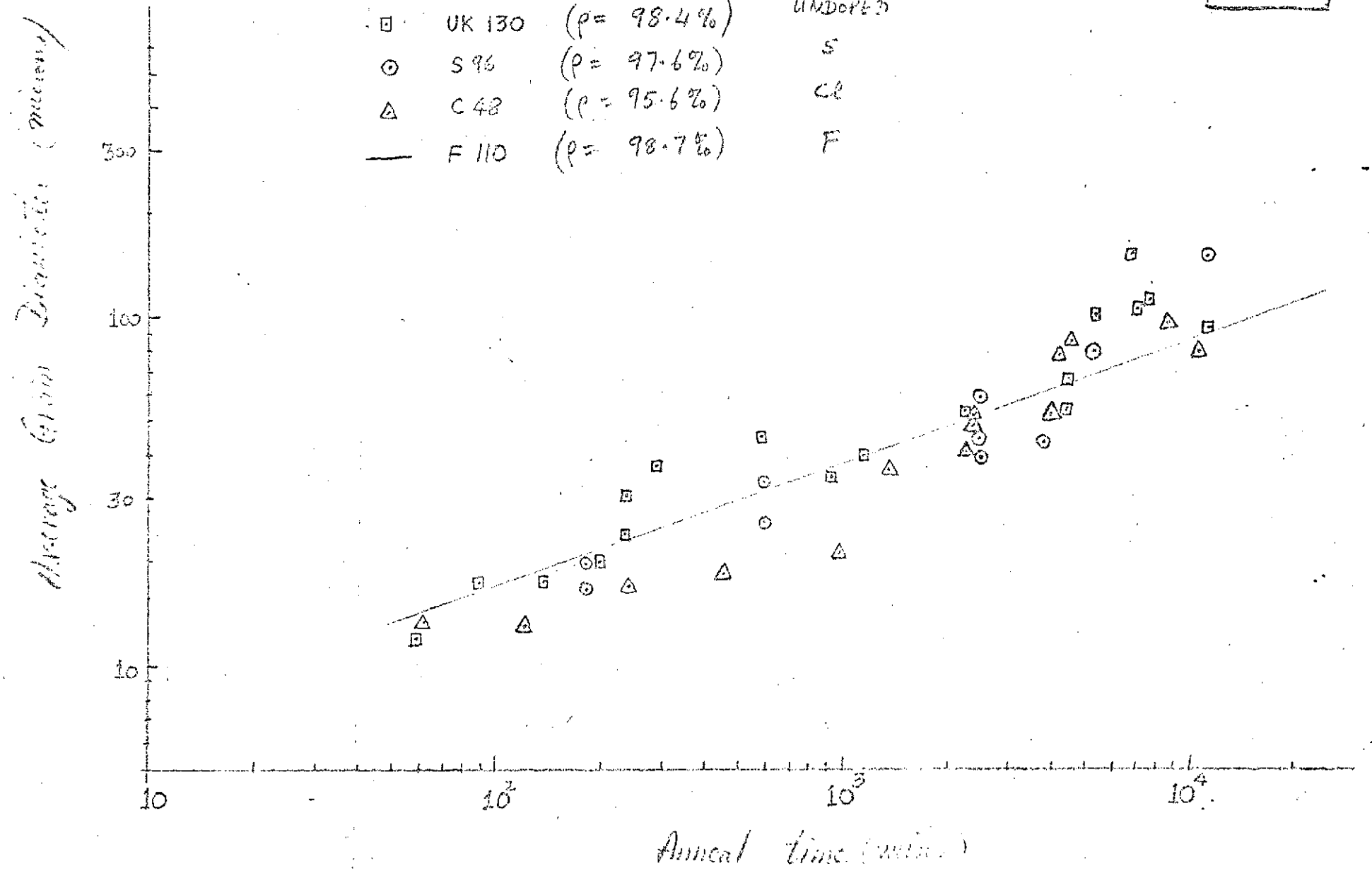

Figure 9a

ANION DOPED : FISHER MgO (1 – 4 % POROSITY)

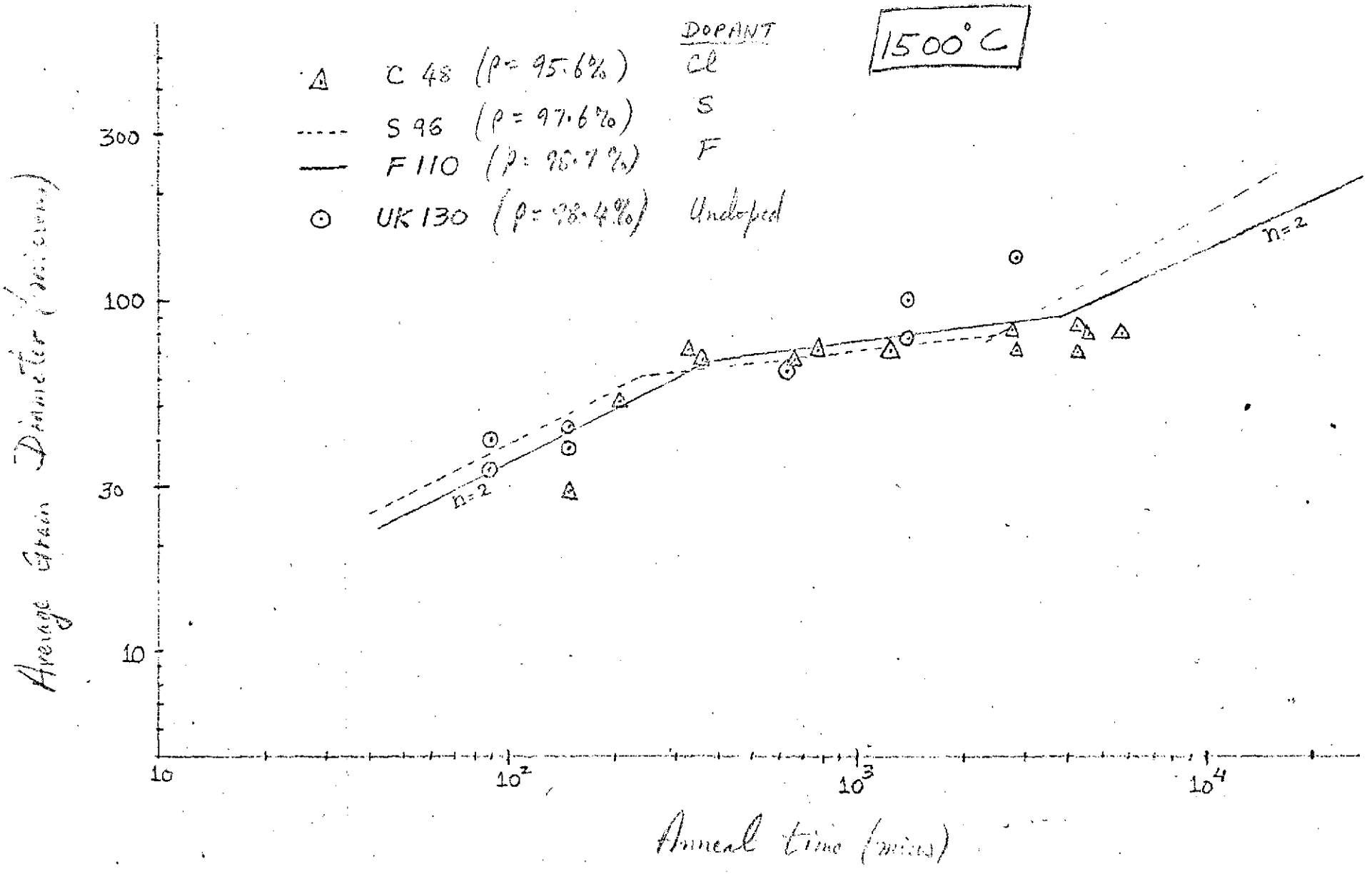

Figure 96

ANION DOPED FISHER Al$_2$O$_3$ (< 1% POROSITY)

1300°C

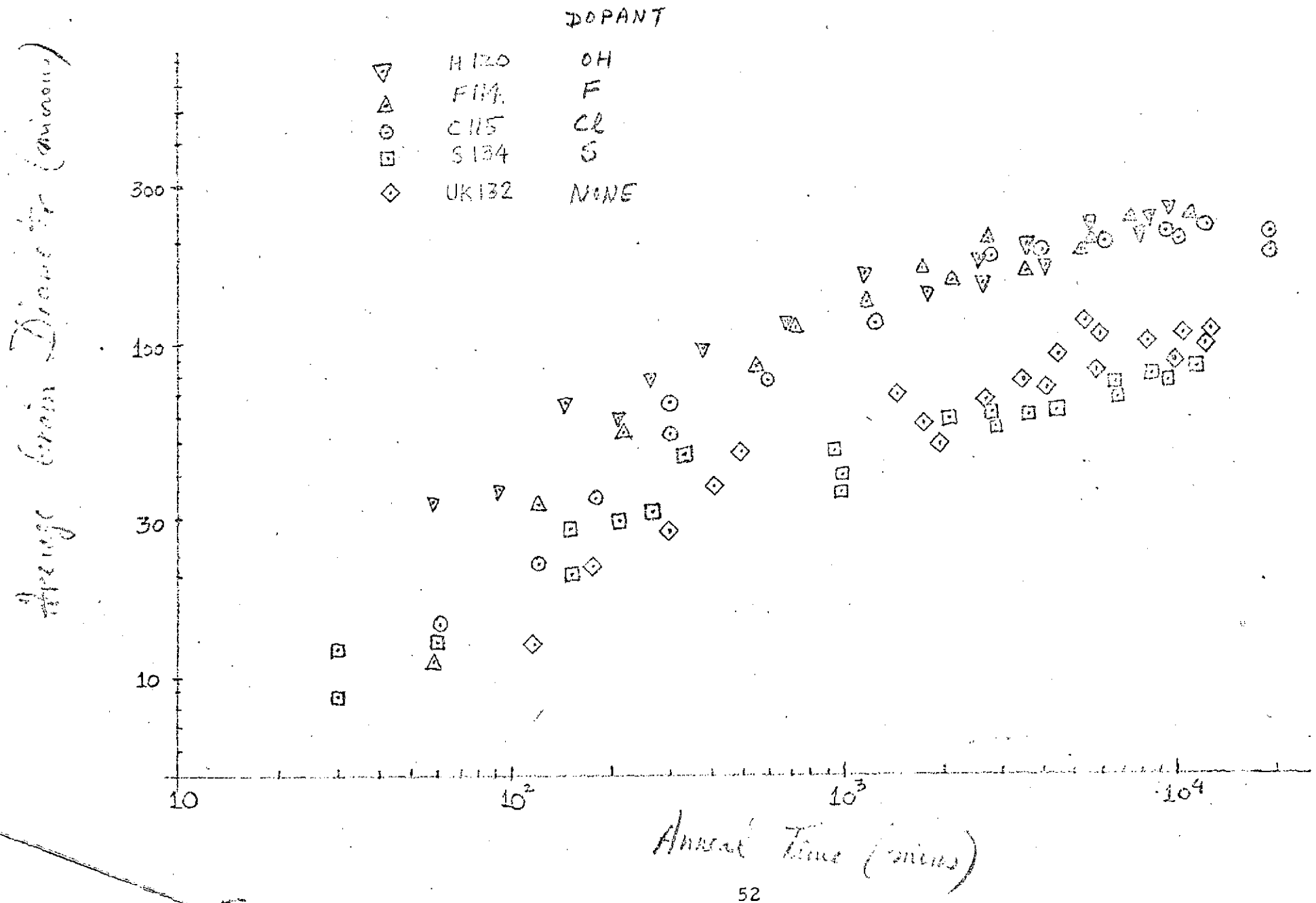

Figure 10a

ANION DOPED FISHER MgO (< ½% POROSITY)

(1500°C)

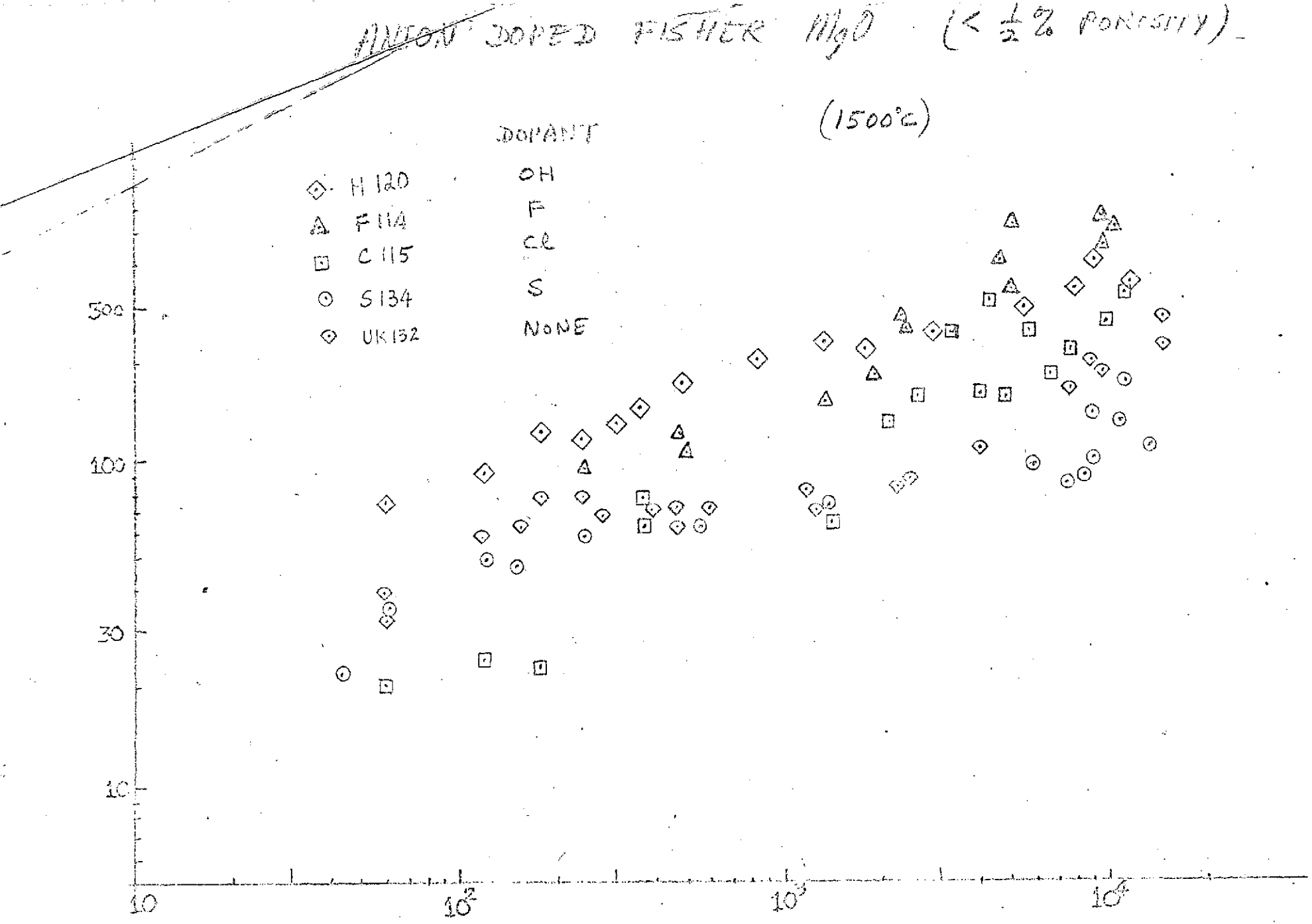

Figure 106